Sol-Gel Chromogenic Materials and Devices

Michel A. Aegerter*

Instituto de Física de São Carlos, Universidade de São Paulo, Caixa Postal 369, 13560-970, São Carlos, SP, Brasil
*Present address: Institut für Nene Materialien – INM, Im Stadtwald, Gebäude 43, D-66123 Saarbrücken – Germany

In the last few years the sol-gel process has turned into an interesting and promising method of synthesizing materials for obtaining thin or thick films with definite functions. The techniques of film preparation such as dip and spin coating are simple and allow us to prepare coatings with smooth optical surfaces with controlled stoichiometry, structure and texture. In this paper we give an up to date overview of what has been achieved in the field of chromogenic materials such as anodic or cathodic electrochromic coatings, counter or ion storage electrodes, transparent electron conductors and ionic conductors to be used in electrochromic (EC) devices. We also review the sol-gel research in the related areas of photochromic, thermochromic and electrooptic sol-gel materials whose properties are essentially used to modulate the luminous or solar energy as well as sol-gel materials prepared in the form of nanoparticles proposed recently for the development of a new type of solar cell. Finally we stress the future developments in these fast growing fields.

1 Objective

The objective of this paper is to give essentially an up to date review of what has been achieved in the field of *Chromogenic Materials and Devices* prepared by the *Sol-Gel Process*. All the references obtained through a STN International File Search (22.3.1994) with keywords sol, gel and electrochromism or photochromism or thermochromism as well as more recent ones are cited so that the reader should have a complete overview of this fast growing field which has gained importance in science as well as in industry during the last few years.

2 Introduction

International interest in solar energy research has strongly fluctuated during the last two decades. It was high during the latter half of the 1970s as a consequence of the oil crisis but faded somewhat in the 1980s. Today it is recognized worldwide that the technologies involved in energy efficiency and solar energy could alleviate the environmental crisis manifested by global heating through the greenhouse effect. The hazardous increases of UV radiation through the holes in the ozone layer also contribute to the pressure to limit use of fossil and nuclear fuels because of their environmental impacts. However this revival is also due to the increasing interest of other specialized markets such as automotive, aerospace, defense, toys, etc. which look very promising at short term, with sales impact exceeding several billion dollars.

A wide class of materials, called *chromogenic* materials, are known to change in a persistent but reversible manner their optical properties such as optical transmission, absorption, reflectance and/or emitance in response to changes in ambient conditions [1].

For instance Cd or Ag doped glasses and organic dye doped polymers or organic dyes incorporated in inorganic porous matrices change their color when exposed to UV or visible light. This *photochromic* property is widely used today in commercial products such as lenses. A few materials, such as VO_2, are known to exhibit an analogous effect when heated at a defined temperature and are known as *thermochromic* materials. Others, called *barochromic* materials, change their color when exposed to a change in ambient pressure; this is exhibited for instance by samarium sulphide. Other devices used *liquid crystals or polymer dispersed* materials incorporated in a liquid; the application of an electric field changes the orientation of these molecules altering the optical absorption or scattering of the layer.

Technologically, however, the most promising chromogenic effect is called *electrochromism* and is defined as the persistent but reversible optical change produced electrochemically. A wide range of materials are known today to

exhibit a reversible coloration by the application of an electric field or more precisely by the passage of an electric current and ions through them. These materials are required to exhibit a mixed electronic and ionic conductivity and consequently are often amorphous and porous to provide an open network for rapid ionic diffusion. A common feature of such materials, unlike the liquid crystals used in displays, is that once the material is colored, the applied voltage can be switched off and the color retained, making the electrochromic (EC) devices more energy efficient.

Commercially, hearing aid battery powdered electrochromic sunglasses and other systems are already on the market. However, owing to the more than 30 million new cars and trucks produced worldwide each year and to the recent advance of technology, in the near future the greatest opportunities for EC technology is without any doubt in the automotive industry [2, 3]. Small to medium area transmissive or reflective EC devices have already been successfully commercialized for automobile rear and side view mirrors (more than one million sold in 1993) and automotive sunroofs.

This success represents the first stepping stone towards large area devices for application in architectural glazing that will allow active optical response to changing environmental conditions. This technology will save on cooling and lighting energy costs and, at the same times, provide glare control and improved thermal comfort as shown in Fig. 1 [4, 5].

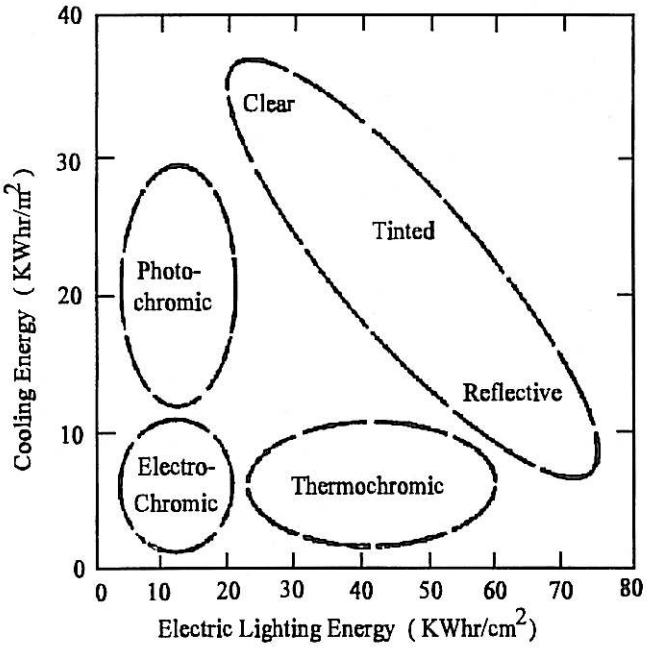

Fig. 1. Schematic diagram of projected cooling and electric lighting energy for a building using different window panes [4]

3 Electrochromic Devices

Electrochromic devices have been classified into several categories depending on their application, their spectral transmission variation or their configuration. Reilly et al. [6] classified *ideal* electrochromic materials into three types according to their transmittance, which could vary typically between 0.1 and 0.8, and switches over different spectral ranges such as the entire solar spectrum, the visible subspectrum only or the solar infrared subspectrum only (Fig. 2). As each of these spectral types could change transmittance by a corresponding change in either absorption or reflection, six basic electrochromic materials can be considered. On the other hand, Cronin and Agrawal [3], in a more pragmatic way, classified the devices according to their configuration. As electrochromism has never been observed in an isolated compound and requires a simultaneous double injection of electrons and ions, the device configuration involves the development of an electrochemical cell consisting of multiple layer stacks that are sequentially deposited or laminated. Figure 3 shows a few typical examples; the simplest device uses a liquid solution between two electronically conductive electrodes (Fig. 3a) and the optical modulation results in a redox reaction at the liquid/electrode interface when an appropriate potential is applied to the conductive electrodes. For transmissive devices both conductive electrodes must be transparent. For large area devices, to improve the safety of the device and to avoid the effect of hydrostatic pressure and the necessity of a seal, the liquid solution can be replaced by a solid-state electrochromic film such as a polymer. In this case the electrochemically active chromophores are incorporated into the matrix by chemical bonding.

More sophisticated configurations are also shown in the figure. These EC systems can be assembled on a glass substrate by sequential deposition where at least one of the coatings is an electrochromic layer (Fig. 3b) or, alternatively (Fig. 3c, d) an electrochromic film can be deposited on a conductive substrate (left part) and then assembled to the other part. All these devices may use a sealed liquid electrolyte as shown in both examples or, as preferred for large area applications, a solid electrolyte. The last system (Fig. 3d) makes use of a counter electrode which serves as an ion storage layer which can also be electrochromic in order to achieve a higher dynamic transmission range. These are only typical examples and modifications can be made in order to improve the performance of the systems for dedicated applications or to take into account the particular conditions of their use. The reader should consult the specialized literature for more insight on these questions [3–5, 7]. The performance factors which will influence the market acceptance of electrochromic windows have recently been reviewed by Selkowitz et al. [5] and Sullivan et al. [8].

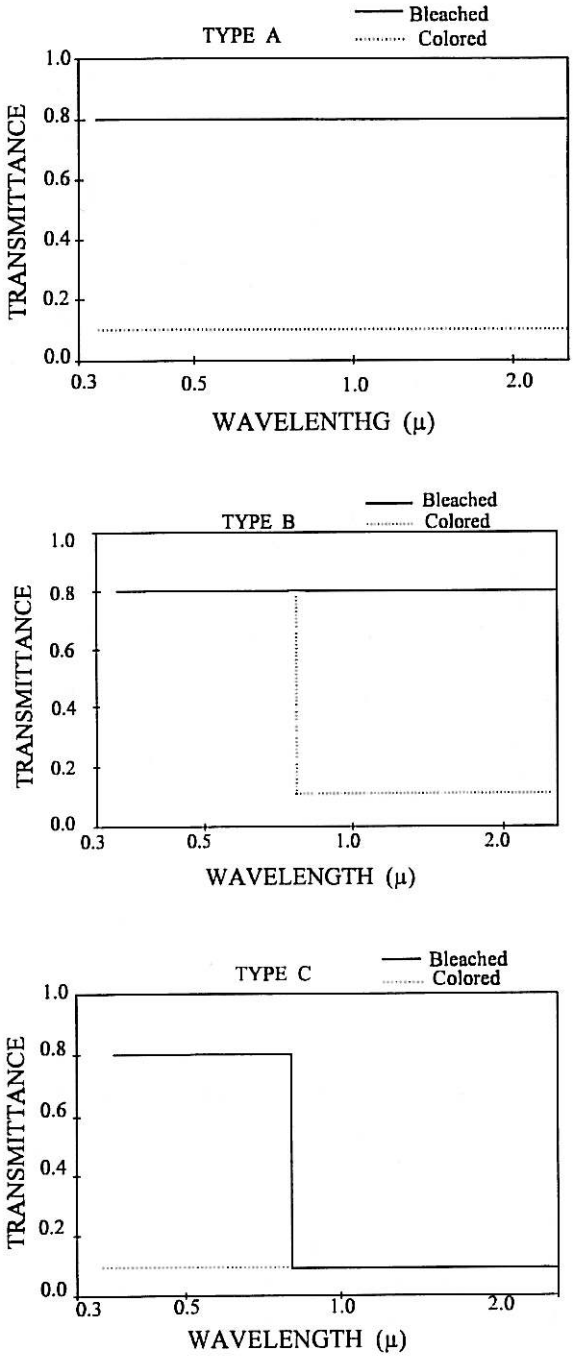

Fig. 2a–c. Ideal electrochromic spectra: **a** uniform switching over the entire solar spectrum; **b** switching over the infrared spectrum only; **c** switching over the visible spectrum only [5]

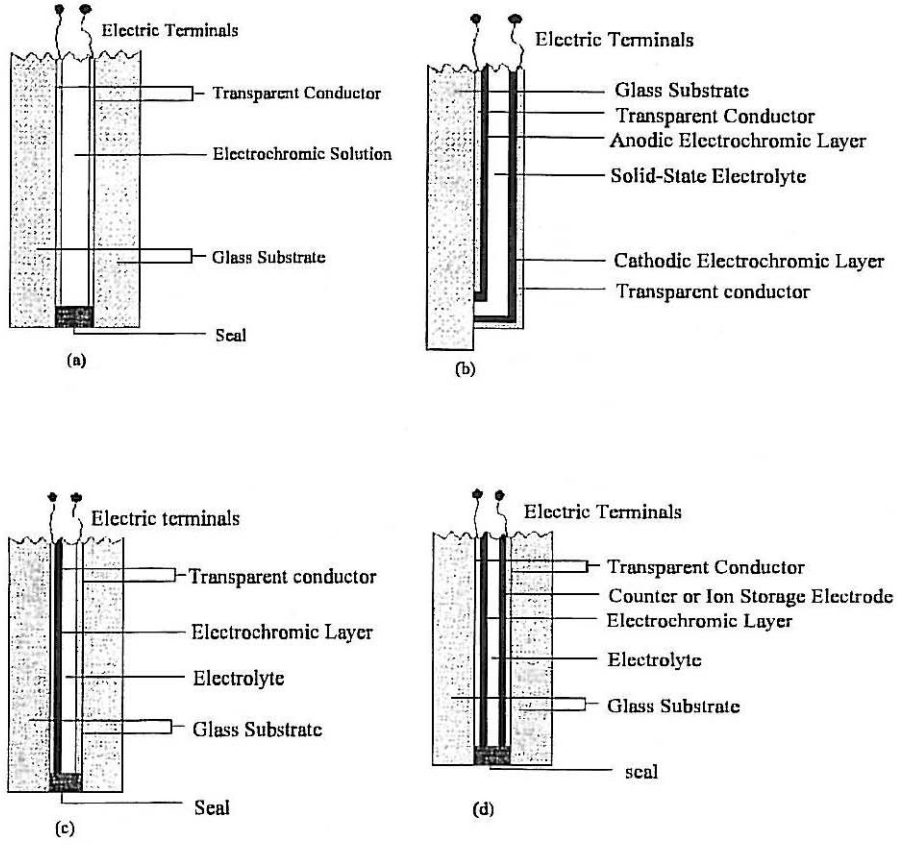

Fig. 3a–d. Typical designs of electrochromic devices [3]: **a** EC device with a liquid solution between two electronically conducting electrodes; **b** EC device which uses an EC thin film and a solid state electrolyte and which can be assembled on one glass substrate by sequential deposition; **c** EC device which uses a liquid or solid electrolyte (without the seal) and an EC coating; **d** EC device similar to **c** but which also uses a counter electrode (ion storage) which could also be electrochromic

4 Materials for Electrochromic Devices

4.1 Overview

Electrochromism has been known since 1953 when Kraus [9] discovered that a vapor-deposited WO_3 layer on a semitransparent metal layer (Cr, Ag) was intensely blue in color when cathodically polarized in 0.1 N H_2SO_4. However world wide research on this topic started only after the fundamental work of Deb [10, 11] on the same material two decades later. Today several other materials are known to exhibit such a property. Most of them are inorganic

oxides of transition metals, to which we shall restrict this review, but several organic materials, mostly doped polymers, have been also discovered [12, 13]. However, despite hundreds of scientific and technical papers, the fundamentals of the phenomenon are still not well understood. Usually the coloration and bleaching of these materials is described schematically by

$$MeO_n + xI^+ + xe^- \leftrightarrow I_xMeO_n \quad (1)$$

where Me is a metal atom, I^+ is a singly charged ion such as H^+, Li^+, Na^+, K^+, Ag^+, e^- is an electron and n depends on the particular type of oxide. Some materials color when they are cathodically polarized, others when anodically polarized and a few of them color in both states. According to Granqvist [14], the electrochromic oxides can be divided into three main groups with regards to their crystalline structure: perovskite-like, rutile-like and layer and block structure, and the general occurrence of MeO_6 building blocks in these materials is of fundamental importance.

A partial list of the inorganic electrochromic materials used to formulate EC devices is given in Table 1 and, for sake of completeness, Tables 2 and 3 list the most important materials which can be used as transparent electronic conductor and electrolyte (H^+ and Li^+ conductors) respectively. In order to be useful for application, these materials should have not only outstanding physical and chemical properties but should also meet severe criteria regarding temperature range, cyclability, corrosion resistance, etc. For a definite application most of them may not yet meet these criteria or meet them only partially. As an example, Table 4 shows the desirable features of an electrochromic automobile sunroof [3]. For other applications some of the requirements are even more stringent [2, 4]. A complete description of device evaluation and test methods can be found in Czanderna and Lampert [15].

4.2 Sol-Gel Materials

Practically all the materials listed in Tables 1–3 were originally prepared by non sol-gel methods such evaporation, DC diode, magnetic or reactive sputtering, electrochemical deposition, etc. and no detailed explanations will be given here. The reader should consult the specialized literature and the references given in the tables should be helpful to start.

The sol-gel process will not be reviewed in this paper as several reference books are available today on this subject [103, 127, 128]. The method appears now to be one of the most promising technologies for preparing coatings with tailored properties [129]. In the field of chromogenic materials, it has until recently been used mainly to develop the chemistry of the precursor sols, showing that the method was adequate to obtain coatings with chromogenic properties. More recently, however, because of its intrinsic advantages over other techniques, which include the use of inexpensive coating equipment for

Table 1. List of inorganic electrochromic materials prepared from sol-gel processes and non-sol processes (only partial list)

Polarization	Material	State	Color	Reference (non sol-gel)	Reference (sol-gel)
Cathodic	WO_3	a, c	blue	[11, 16]	[3, 17–33]
Cathodic	K_xWO_3	c	blue	[34]	
Cathodic	WO_3–TiO_2	a	blue	[35]	[35]
Cathodic	WO_3–MoO_3				[36]
Cathodic	MoO_3	a, c		[37]	[38, 39]
Cathodic	CeO_2		UV		[35, 40, 41]
Cathodic	CeO_2–SnO_2				[41]
Cathodic	CeO_2–TiO_2	c,*	UV		[40, 42–50]
Cathodic	TiO_2		grey	[51, 52]	[53–58, 77]
Cathodic	TiO_2–Al_2O_3		blue		[53]
Cathodic	TiO_2–Cr_2O_3		blue		[53]
Cathodic	TiO_2–WO_3				[57, 59, 60]
Cathodic	TiO_2-viologen				[58]
Cathodic	Nb_2O_5	a, c	a-brown c-blue	[61–65]	[42, 55, 56, 66–74]
Cathodic	Fe_2O_3				[91–93]
Cathodic	Fe_2O_3–TiO_2				[92, 93]
Cathodic	Fe_2O_3–SiO_2				[92, 93]
Cathodic	SnO_2	*			[94]
Both	V_2O_5	c	green, yellow, red	[75, 76]	[39, 54, 75, 77–80]
Both	V_2O_5–Na_2O				[81, 82]
Both	V_2O_5–Ta_2O_5	powder	grey		[83]
Both	V_2O_5–Nb_2O_5	powder	grey		[83]
	V_2O_5–TiO_2	a	blue, green, yellow, reddish-brown		[84]
Anodic	IrO_2			[85]	
Anodic	NiO			[86, 87]	
Anodic	$Ni(OH)_2$			[88]	
Anodic	$Fe_4(Fe(CN)_6)_3$			[89]	
Both	Rh_2O_3			[90]	

[a] Amorphous
[c] Crystalline
* More useful for counter electrode

Table 2. Partial list of inorganic transparent conductors used for the fabrication of EC devices (reference non sol-gel [95–97])

	Materials Reference (sol-gel)
In_2O_3:Sn (ITO)	[98–100]
SnO_2	[101–110]
SnO_2:Zr	[107]
SnO_2:Ti	[107]
SnO_2:Sb	[111]
SnO_2:F	
V_2O_5	[112]
ZnO:Al	
Au (thin film)	

Table 3. Partial list of inorganic and organic electrolytes

H^+	Li^+	Reference (non sol-gel)	Reference (sol-gel)
Ta_2O_5		[113–115]	[116, 117]
ZrO_2		[114]	
$HU_2PO_44H_2O$		[118, 119]	
SiO_2		[52]	
Aminosil (SiO_2)			[120]
ORMOCER-TiO_2	ORMOCER-TiO_2		[121]
Sol-Gel Polymer PBSS			[122]
PWA-TiO_2			[59]
HPA-SiO_2			[59]
	Li_3N	[123]	
	$LiAlF_4$	[124, 125]	
	$LiNbO_3$	[124]	
	$LiTiO_3$	[124]	
	$LiAlSiO_4$	[126]	
	Nasicon		[145]
	Li_2O–SiO_2–P_2O_5		[148, 154]
	$(LiCl)_2$–R_2O_3–SiO_2		[151, 152, 155–157]
	V_2O_5		[159]
	ORMOLYTE		[160]

Table 4. Desirable features for an electrochromic automobile sunroof [3]

Luminous Transmission Range	< 10% in colored range > 50% in bleached state
Solar Transmission	< 10% in colored state
Response time	< 15 min. to achieve 90% of coloration or bleach
Temperature Range	− 40 to 100 °C
Cyclic Durability	> 20000 cycles
Lifetime	> 5 years
Others	Solid state, low power consumption, low cost

coating small and large areas, and especially its applicability to design chemically the molecular precursors to better control the texture and structure of the films [129, 130], this method was used to develop better oxide coatings and even new coatings with properties which have never been obtained previously. EC devices built partly or entirely with sol-gel materials have been extensively tested since 1991.

In the next sections each group of sol-gel materials is reviewed separately.

4.3 Sol-Gel Electrochromic Coatings

The oxide coatings which have been prepared by the sol-gel process and whose electrochromic characteristics have been reported and discussed involve practically eight groups: WO_3, MoO_3, TiO_2, Nb_2O_5, V_2O_5, CeO_2, Fe_2O_3 and SnO_2 and mixed compounds of these materials.

An extensive review on the same subject has been produced by Agrawal et al. [131]. Limited descriptions of some topics have also been given [29, 78, 132–134].

4.3.1 WO_3 and WO_3 Doped with TiO_2 or MoO_3

WO_3. WO_3 is the most studied electrochromic material and is considered today the best for EC applications. It is a cathodic EC material and it changes its color from transparent or yellow to deep blue with a large optical modulation when it is reduced by H^+ or Li^+:

$$WO_3 + xM^+ + xe^- \rightleftharpoons M_xWO_3 \tag{2}$$

where $M^+ = H^+$, Li^+, etc.

The bronze can also be formed when sodium, potassium or silver are used. However as the size of the ions increases the rate of diffusion decreases, diminishing the rate of optical modulation [17, 18].

At least four basic sol-gel routes have been developed for the preparation of the WO_3 sols:

1) acidification of sodium tungstate [19–21];
2) use of peroxypolytungstic acid [22–25];
3) hydrolysis of alkoxides [22, 26–28];
4) reaction of tungsten chloride and oxychloride with alcohols [30, 32, 39, 135].

The first method is one of the earliest efforts to produce sol-gel WO_3 films and its major advantage is the formation of WO_3 at room temperature with no formation of decomposition products. It is therefore possible to produce thick and unstressed films. However the stability of the solutions (which is an important parameter for industrial production) and the adhesion of the coatings to the substrate were found not to be adequate, although the sol stability could be slightly improved by complexing it with appropriate additives such as dimethysulfoxide [20].

In the second method, tungsten and tungsten carbide powder are digested by an aqueous solution of hydrogen peroxide. The product, a peroxytungstic acid, is isolated and then dissolved in a polar solvent such as alcohol or water. The acid is decomposed into tungsten oxide during the heat treatment of the film at low temperature (100–200 °C).

The tungsten alkoxide (third method) is the classical sol-gel route for any kind of oxide but is expensive and consequently not useful for industrial application. Crack-free films could only be prepared with small thickness (< 50 nm). It is therefore necessary to repeat the deposition process to obtain thicker films to get a sufficient optical contrast.

According to Livage [29] the reaction of tungsten oxy-chloride ($WOCl_4$) with isopropanol is the best method of preparation as it is a cheap technique and

leads to a sol that is stable for several months because of the formation of molecular oligomeric species $(WOCl_{4-x}(O^iPr)_x)_n$ [30]. In this method, tungsten chloride is reacted with an anhydrous alcohol and the resulting material is diluted with more alcohol to obtain the precursor sol. The films have a high uniformity, better than those prepared via a colloidal route. The same precursor has also been used to deposit WO_3 by spray pyrolysis [31]. Micrometer-thick hydrated films of composition $WO_3 \cdot nH_2O$ are easily obtained, with the control of the amount of water and adequate heat treatments controlling the film morphology, essential for these applications. The electrochromic properties were found to be dependent upon the values of n. It was also found that the switching time and the long term memory decrease when the amount of water increases due to faster ion diffusion through the gel network [32]. When Li^+ ions are used the best electrochemical stability was encountered for $n = 0.5$ as higher amount of water leads to a gradual decrease of the current, an indication of the occurence of an irreversible process [21].

Finally two recent interesting results concerned with the improvement of WO_3 have appeared. Cronin et al. [3, 18] have patented the preparation of a WO_3 electrochromic coating solution prepared by reacting metallic W with a mixture of a peroxy acid such as hydrogen peroxide and an organic acid such as acetic or propionic acid at between -10 and $+12\,°C$ for 16–26 h. The resulting product, a W-peroxy acid, was then esterified by reacting with low boiling one to three carbon alcohol to produce a peroxyester-W derivative (PTE). The sol was found to be stable if stored below 10 °C. The deposited coating was converted to an electrochromically active layer by removing the volatile organics by firing at a temperature as low as 100 °C. It is claimed that the optical transmission of the coatings prepared in accordance with the disclosures decreases from 85% to less than 15% in a matter of seconds. Higher firing temperatures will only increase the film density, making the film tougher and more resistant to scratching. Such a method can be extended to other transition metals such as Mo, Mn, Cr, Rh, Ir, Ni, etc. Due to the low temperature of the film heat treatment, it is without doubt an important technique for obtaining films for industrial applications.

Denesuk et al. [33] have presented a novel synthesis of a sol-gel WO_3 precursor which produces films with different microstructures. The precursor sols were prepared using the above method in anhydrous ethanol in which was added 32 mol% oxalic acid dihydrate (referenced to the W-metal content in PTE). The coatings, prepared by the dip-coating method, were heat treated at 250 °C in ambient atmosphere. The films prepared without the addition of oxalic acid were homogeneous and amorphous. Those prepared with the oxalic acid had an inhomogeneous amorphous/crystalline hybrid structure (with no remaining trace of the additive) and contained small (~ 5 nm) regions of increased electron density. The optoelectrochemical data indicate that the intercalation capacity and the dynamic optical efficiency of these hybrid films are much larger and essentially independent of cycling (Fig. 4).

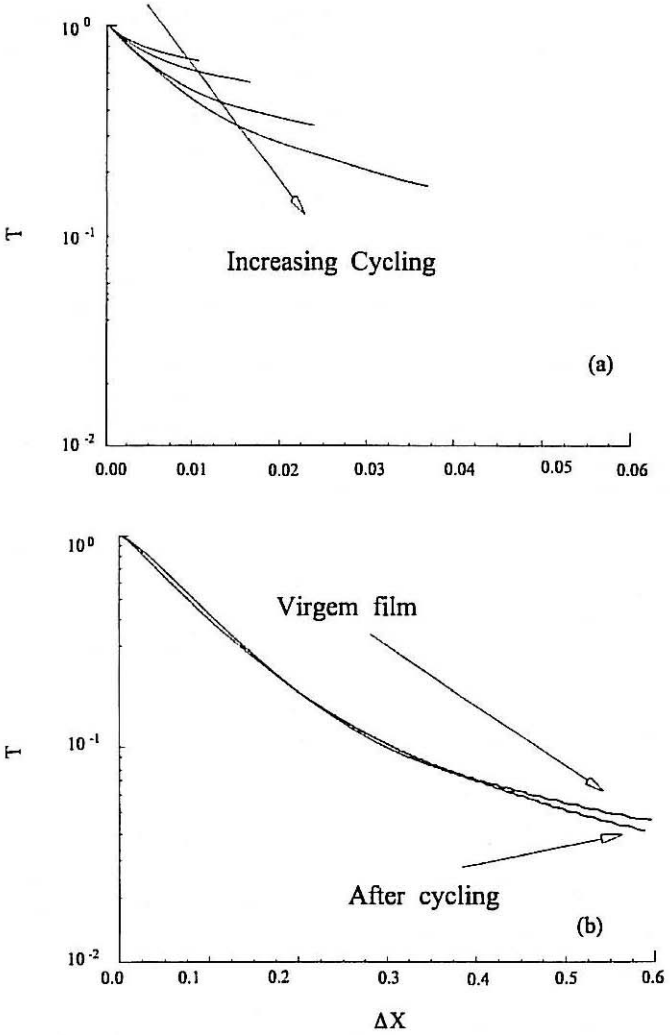

Fig. 4a, b. Log-linear plot of the transmission T vs the change in intercalation Δx for a WO_3 film: **a** prepared without oxalic acid dihydrate; **b** prepared with 32% of the same additive. In **a** one observes a strong cycling effect while in **b** the effect does not exist. This latter film possesses a larger average optical efficiency than the former [33]

These two last results are especially promising for the preparation of commercial EC products and show that the sol-gel method has now reached a state of the art such that it may supplant conventional technologies.

WO_3–TiO_2. Using a sol prepared with a mixture of tungsten chloride (WCl_6) tetraisobutylorthotitanate ($Ti(OBu)_4$) and ethanol, stable for weeks, Göttsche et al. [35] have claimed a better electrochemical stability under Li insertion for

films dipped four times (thickness ~150–190 nm) and then tempered in air at 200 °C for 1 h (the same property has also been found in sputtered deposited films). However, the addition of TiO_2 (up to 50 mol%) was found to reduce the number of tungsten active sites and to lead to a decrease in the reversible optical transmittance variation with a corresponding reduction of the coloration efficiency from about 70 cm^2/C for an undoped film to 35 cm^2/C for a 33% Ti doped one. On the other hand, the incorporation of Ti was found to prevent the crystallization of tungsten oxide so that the films can be solidified at higher temperatures. The addition of 10–15 mol% of TiO_2 resulted in coatings with maximum cyclic lifetimes.

WO_3–MoO_3. WO_3–MoO_3 films have been deposited from colloidal solutions prepared by mixing H_2WO_4 and H_2MoO_4. After filtration through a cation-exchanger column, the sol was kept at a constant temperature to promote the polymerization [36]. A blue shift of the absorption band compared to pure WO_3 was observed which was maximum for a molar ratio W: Mo of 7.3.

4.3.2 MoO_3

This compound also forms a number of bronzes with alkali metals. It colors when reduced by ion insertion but its ability to color is lower than that of WO_3. Sol-gel MoO_3 has been prepared by Moser and Lynam [39] using halogenated compounds as precursors. Wang et al. [38] have used molybdenum chloro-ethoxide as precursor hydrolyzed in water with a mole ratio H_2O/Mo of two to four. The films were found to be amorphous below 350 °C. At higher temperatures the films crystallized in air into MoO_3. At 600 °C Mo_9O_{26} was also found and other oxides were found if the heat treatment were made under Ar atmosphere or vacuum.

4.3.3 TiO_2 and TiO_2 Doped with Al_2O, Cr_2O_3, WO_3 or Coated with Viologen

TiO_2. Such coatings have been prepared from the classical alkoxy route by Doeuff and Sanchez [53], Nabavi et al. [54], and Ozer et al. [55, 56]. The last authors have prepared amorphous gel coatings by a spin coating technique by using a drop of Ti $(OBu)_4$–BuOH solution. When amorphous ($T < 400$ °C), the insertion of Li^+ ions was found to occur at random and no peak was observed in voltammetry but instead a continuous reduction and oxidation curve was obtained. After heating to 400 °C the films were found to be crystalline (anatase) and the voltammograms for Li insertion (20 mC/cm^2) showed two cathodic and anodic waves corresponding to defined sites in the TiO_2 structure. In both cases the color-bleaching cycles were reversible. In pure compound the color was grey but was blue for doped materials (Al, Cr). Ozer et al. [55], using sols prepared

with Ti $(isoPrO)_4$, Ti $(isoBuO)_4$ and acetic acid as catalyst, have found that the coatings were electrochromic under certain preparation conditions.

Bell et al. [57] have also reported electrochromism in a film of pure TiO_2 prepared from a sol made with Ti isopropoxide and ethanol or isopropanol, showing a neutral greyish color under Li insertion.

TiO_2 gels have also been synthesized from modified alkoxide precursors using acetic acid which is known to slow down the hydrolysis-condensation process of Ti alkoxides and thereby preventing precipitation [77]. The electrochemical and electrochromic properties of 0.5-μm thick film prepared in this way are quite similar to those obtained without acetic acid, but their color was found to be blue instead of grey. This was attributed to the presence of some acetate groups which remained bounded to the metal. The ligand field around the titanium is therefore different and changes the color. The presence of impurities or organic groups may therefore change the cosmetic aspect of the film after ion insertion and may be a tool to adjust the color of the coating in the colored state.

A new approach has recently been proposed by Hagfeld et al. [58]. Thick (3.5–4 μm) coatings of *nanocrystalline* TiO_2 particles (which can easily be prepared by the sol-gel process [103]) have been made by spreading a paste of 15-nm size colloidal TiO_2 on SnO_2:F conducting glass. After autoclaving at 200 °C and firing at 450 °C in air for 30 min the films were found to be crystalline with the anatase crystal structure. These films are highly porous from the outer layer to the conducting back contact with a roughness factor of 540. Cyclic voltammetry performed in $LiClO_4$/acetonitrile electrolyte shows a cathodic and anodic peak and the charge stored during the intercalation process was very high, 0.11 C/cm^2 for both the forward and reverse scan showing that the

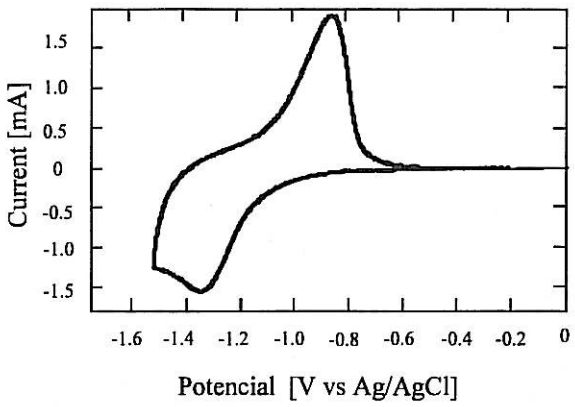

Fig. 5. Cyclic voltammetry of a transparent nanocrystalline TiO_2 electrode. Charge passed is $Q_{cathodic} = 0.11$ C/cm^2 and $Q_{anodic} = 0.11$ C/cm^2. The film thickness is 3.5 μm and electrode area 1 cm^2. Ar purged 1 mol/l $LiClO_4$ in acetonitrile is used as electrolyte. The reference electrode is Ag/AgCl (sat. KCl in water) and the counter electrode is glassy carbon. Voltage is scanned from 0 V to − 1.50 V to 0 V at a scan rate of 5 mV/s [58]

intercalation is strictly reversible (Fig. 5). The Li^+ insertion is accompanied by an intense color change from transparent to dark blue as shown in Fig. 6, which develops in about 25 s after the application of a step potential. On switching back the potential to the initial potential value, the coloration disappears on the same time scale. Stability tests performed with a sample of 0.44 cm^2 geometric area show a decline of the cathodic wave of $\sim$ 25% during the first three cycles. No other change had been observed in up to 110 cycles.

This behavior contrasts with that of anatase films prepared by conventional methods which are unable to intercalate Li ions to any significant extent. Apparently the nanoporous morphology of these new devices greatly facilitates the reversible Li intercalation.

This recent investigation establishes the advantage of using nanocrystalline coatings for Li^+ intercalation due to the unique morphology and surface structure of the coating.

TiO_2:Al_2O_3. Doeuff and Sanchez [53] have also reported some properties of TiO_2 doped with aluminum. This dopant was introduced in the colloidal titanium sol in the form of aluminum-*sec*-tributylate ($Al(OBu^s)_3$). The films, heat treated at 400 °C for 2 h, were slightly green-brown but transparent. Under Li^+ insertion they turned blue due to a large unstructured optical absorption band centered at 750 nm probably caused by intervalence transfer between Ti(III) and Ti(IV). This is in agreement with ESR measurements which confirm the presence of Ti^{3+} in distorted octahedral symmetry in the reduced compound. The change in color, grey for pure TiO_2 to blue for doped TiO_2, is attributed to the modification of the localization of Ti^{3+} due to the coulombic field created by the impurity.

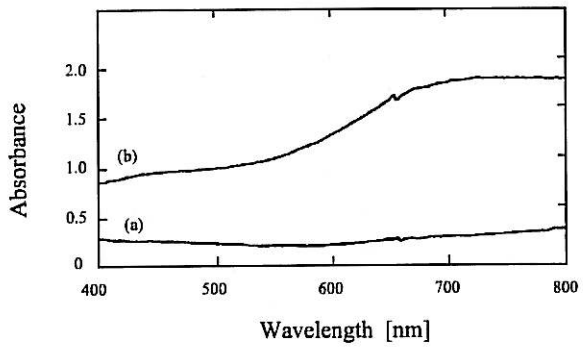

Fig. 6. UV-VIS observed during electrochromic switching of nanocrystalline TiO_2. *Line a* – bleached state (– 0.64 V vs Ag/AgCl); *line b* – colored state after polarizing to – 1.64 V vs Ag/AgCl for 10 s. 1 mol/l $LiClO_4$ in acetonitrile, film thickness 3.5 μm. The observed background absorption in the bleached state is due to light scattering. Then, 10 s after applying the potential step, the absorbance increases to a value above 1 in the whole visible region with a broad maximum of absorbance close to 2 in a wavelength interval of 660–880 nm. Charge passed in 0.10 C/cm^2 [58]

TiO_2:Cr_2O_3. The same authors [53] also reported similar conclusions with Cr^{3+} doping.

TiO_2–WO_3. Dip coated films containing 0–100% WO_3 have recently been prepared by Bell et al. [57] from precursors containing Ti isopropoxide or Ti propoxide diluted in ethanol and a tungsten alkoxide precursor. The films have been fired in air at 300 °C. The results are in general agreement with those obtained by Göttsche et al. [136] with respect to the coloration performance of the mixed WO_3:TiO_2 films. They exhibit coloration by absorption. The authors found that the absorption decreases with the TiO_2 content but that the bleaching was improved at the same time. A wide range of composition (at least 67–100 mol% W) gives a good coloration efficiency. The color of these films is somewhat different from that found in pure WO_3 due to the presence of an additional absorption band in the 2.2–3.2 eV range. They have a more greyish appearance in the colored state.

Recently Stangar et al. [59] have incorporated phosphotungstic acid $H_3PW_{12}O_{40}.xH_2O$(PWA) to TiO_2 xerogel with a ratio PWA/Ti = 7:100. This compound is known as an electrochromic and ion conductor material and belongs to a large family of heteropoly compounds of high molecular weight with Keggin structure of the anion. The optical density change was only about 40% in the visible due to a large structureless band having its maximum in the UV region and decreasing slowly at longer wavelength. The maximum amount of injected proton was 25 mC/cm^2 and the kinetics was slow. However, this compound has interesting properties. Since protons are already present in the PWA structure there is no need for an additional ion conductive material to be in close contact with the electrochromic material to produce its coloration (Fig. 3b). Therefore the layer can be reduced at the transparent conductor (SnO_2:F) interface and oxidised at the PWA/counter electrode interface. However the main drawback is its strong acidity and solubility in water and some organic solvents, which should limit its use for commercial products.

TiO_2-Viologen. An interesting approach has recently been proposed by Hagfeld et al. [58]. Instead of using a doped material, the authors have coated TiO_2 nanoparticles with viologen attached to them by carboxylic groups. These organic compounds have a low redox potential, show significant reversibility, exhibit in the visible a large change of the extinction coefficient following reduction, and possess a first reduction potential that is essentially pH independent. Figure 7 shows the UV-Visible spectral change observed for such a system having a high coloration efficiency of 85 cm^2/C. Stability tests indicate a gradual decrease of the charge exchanged which levels after about 100 cycles to about 75% of the initial value. This new approach looks promising as it combines the effect of a large active area obtained by the use of nanosize particles with the electrochromic properties of organic molecules.

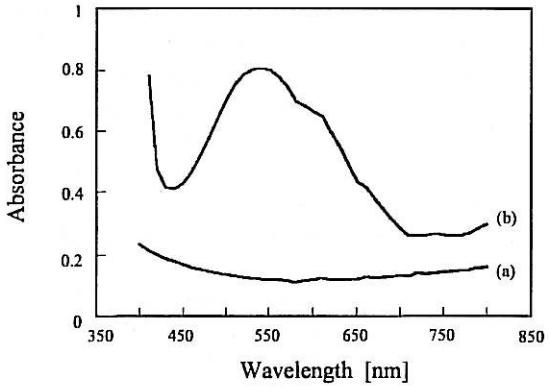

Fig. 7. UV-VIS spectral changes observed during electrochromic switching of a viologen coated nanocrystalline TiO_2 electrode. *Line a* – bleached state under open circuit condition; *line b* – colored state after polarizing to -0.86 V. 0.1 mol/l $TPAClO_4$ in propylene carbonate is used as electrolyte and the electrode area is 1.0 cm^2. The observed background absorption in the bleached state is due to light scattering. Charge passed during coloration is 8.0 mC/cm^2 [58]

4.3.4 V_2O_5 and V_2O_5 Doped with Na_2O, Nb_2O_5, Ta_2O_5 or TiO_2

V_2O_5. The vanadium oxides exist in different stoichiometry, but V_2O_5 is the most used for EC devices. Since the change in the optical spectrum is not as large as in WO_3, it has been used mainly as ion storage electrodes in conjunction with WO_3 as the electrochromic layer, or as electrodes in electrochemical energy storage systems [80]. The reversibility for Li^+ ions is good and is better when V_2O_5 is in the crystalline state [75]. These coatings are yellow in the transparent (bleached) state and therefore slightly reduce the maximum light transmission.

V_2O_5 electrochromic gels have mainly been synthesized by Livage's group using the alkoxy route [54, 77, 78] and by Yoshino et al. [79] using, for instance, alkoxy vanadate $VO(OAm^t)_3$ hydrolyzed with an excess of water. The chemical structure of the precursors ($VO(OAm^t)_3$ and $VO(OPr^i)_3$) have been studied by ESR by Nabavi and Sanchez [137]. The nature of the final material was found to depend on the hydrolysis ratio H_2O/V. For a ratio smaller than three the alkoxy ligands are not all hydrolyzed, leading to the formation of oxy polymers in which organic groups remain bonded to vanadium. These gels exhibit an orange color and give rise to transparent films when dried at room temperature [77]. With higher ratio (H_2O/vanadium > 100) the layer (0.5 μm thick) is mainly a hydrous oxide gel (V_2O_5 1.8 H_2O) with a pale yellow color. The gels have mixed electronic and protonic conductivity and Li ion insertion was found to be reversible.

The study of the structure of these gels shows that the material is made from V_2O_5 ribbons separated by solvent molecules where the vanadium ions are in a square pyramidal environment; the structure inside the ribbons is close to that observed in orthorhombic V_2O_5. When the colloidal solution is deposited on

a substrate, the layers are found to be anisotropic due to the turbostratic stacking of the ribbons perpendicular to the substrate. The electrochemical insertion of Li^+ is reversible, showing two peaks for reduction and oxidation, a behavior which indicates that Li^+ insertion occurs at rather well defined sites and not at random as in an amorphous oxide. After insertion the layers are green due to a broad absorption band whose maximum is at about 1450 nm, typical of intervalence transfers between V^{4+} and V^{5+}, and the kinetics of the coloring and bleaching is fast (a few seconds). Using thicker films (about 10 μm) such devices show multiple colors, turning red to yellow to green.

Alkoxyhalides of vanadium have also been used [39]. In this method vanadium trifluoride oxide, vanadium oxytrichloride or vanadium tribromide have been reacted with an anhydrous alcohol. The fluorinated precursor gave the largest optical modulation.

V_2O_5–Na_2O. $Na_{0.32}V_2O_5$ bronzes have been reported by Pereira-Ramos et al. [82] and Bach et al. [81]. A colloidal solution of V_2O_5 was first prepared using an alkoxy route. Then the solution was passed through an ion exchange column to incorporate sodium. Unlike pure V_2O_5 these materials were found to have a 3-D tunnel structure enabling them to insert Li^+ and Na^+ ions by diffusion without structural change.

V_2O_5–Nb_2O_5. $NbVO_5$ bronzes have been prepared by Amarilla et al. [83] from solutions of vanadyl tri-*tert*-butoxide and $NbCl_5$ in isopropyl alcohol. Li^+ extraction and insertion was verified chemically on powders. The bronzes change their color from yellow to dark grey on reduction.

V_2O_5–Ta_2O_5. The same route was used to obtain $TaVO_5$ bronze [83]

V_2O_5–TiO_2. Mixed V_2O_5–TiO_2 thin coating have been prepared by Nagase et al. [84] from sols prepared from a mixture of $VO(O\text{–iso–}C_3H_7)_2$ and $Ti(O\text{–iso–}C_3H_7)_4$ alkoxides diluted in isopropanol. The sol was stabilized by the addition of acetylacetone and excess of acetic acid. Dip coated films present an electrochromism which is strongly dependent on the atomic ratio $x = Ti/(V + Ti)$ and the calcination temperature. After heat treatment at 400 °C for instance, a two step coloration blue ↔ green ↔ yellow for $0 < x < 0.17$ was observed, while Ti rich coatings ($0.60 < x < 0.67$) exhibited a reddish brown color at potential − 0.8V vs SCE attributed to the presence of V^{3+} ions. The coatings were essentially amorphous with small crystallites of TiO_2 (anatase). At 500 °C the coatings were found to have properties similar to pure V_2O_5.

4.3.5 Nb_2O_5

Sol-gel Nb_2O_5 films are new, very promising candidates for electrochromic coatings. Very few studies have been reported on the electrochromic properties

of Nb_2O_5. Reichman and Bard [61] showed the occurrence of such effects with a 15-μm thick coating produced on the surface of a niobium metallic disk by heating at ~500 °C for about 10 min. A coloring effect, chemically stable and with fast kinetics (1–2 s), was seen in reflexion under either H^+ or Li^+ insertion. Gomes et al. [63, 64] have studied in detail the protonic electrochromic properties of 20-μm thick opaque coating prepared in the same way and Alves [65] has confirmed the possibility of inserting Li ions in a 1-mm thick Nb_2O_5 ceramic prepared from commercial CBMM powder sintered at 800 °C.

The first attempt to fabricate sol-gel Nb_2O_5 for electrochemical purpose has been reported by Lee and Crayston [66] who have spin coated an ITO coated glass electrode with a mixture of $NbCl_5$ dissolved in EtOH. Hydrolysis and gelation were completed in 1 mol/dm^3 H_2SO_4 solution. After drying at room temperature the result was a 5–10 μm thick film with substantial cracking (10-μm islands) and peeling due to important shrinkage. Cyclic voltammograms in $LiClO_4$–MeCN electrolyte showed a blue coloration with a fast coloration (~6 s) and bleaching (~3 s) kinetics and a 6 cm^2/C coloring efficiency. However the durability of the electrochromic response was only a few cycles. The quality of the film has been slightly improved by adding a trialkoxysilane (Glymo) to the precursor sol in order to obtain a Nb–Si Ormocer. Recently Faria and Bulhões [67] have prepared niobium pentoxide films 2.8-μm thick dip-coated on ITO glass from a sol made by dissolving 40 wt% citric acid in 60 wt% ethylene glycol at 60 °C to which was added $NH_4H_2\{NbO(C_2O_4)_3\}3H_2O$. Under Li insertion the films showed a blue color with a transmission change of 82 to 30% at 631.8 nm (5 mC/cm^2).

Colloidal Nb_2O_5 sols have been prepared in Aegerter's laboratory [68, 71–74] using an alkoxide route. Pentabutoxide of niobium ($Nb(OBu^n)_5$) was first synthesized following the Na process described by Mehrotra [138] for other metals. This precursor was then mixed with glacial acetic acid (CH_3COOH) with molar ratio 1/2 resulting in a sol stable at room temperature for several months. The size distribution of the sol particles measured in a light scattering experiment has a z average mean of 16.7 nm. The films had an excellent microstructure with no cracks and defects even at the microscopic scale. They were found to be amorphous up to ~520 °C and after Li^+ insertion their color was brown. At 560 °C the material is crystalline and its structure was identified as the TT phase corresponding to $Nb_{16}O_{38}X_4$ or $Nb_2(OX)_{5+n}$ in which some oxygen atoms have been replaced by other monovalent species such as OH^-, Cl^-, vacancies, etc. The electrochemical properties, tested with 250-nm thick films up to 2000 voltammetry cycles indicate that the cycles are reversible with a maximum charge inserted of 22 mC/cm^2 corresponding to a change in transmission of 80 to 20% in the optical range 400–1200 nm. The color of the coating is deep blue, similar to WO_3 (Fig. 8). No variation of the charge has been noted. The kinetics is rapid, of the order of a few seconds for bleaching and coloring. Protons were also inserted but the lifetime of the coatings did not exceed a few hundred cycles due probably to corrosion problem at the interface EC layer-electrolyte. These new sol-gel coatings of excellent optical and electro-

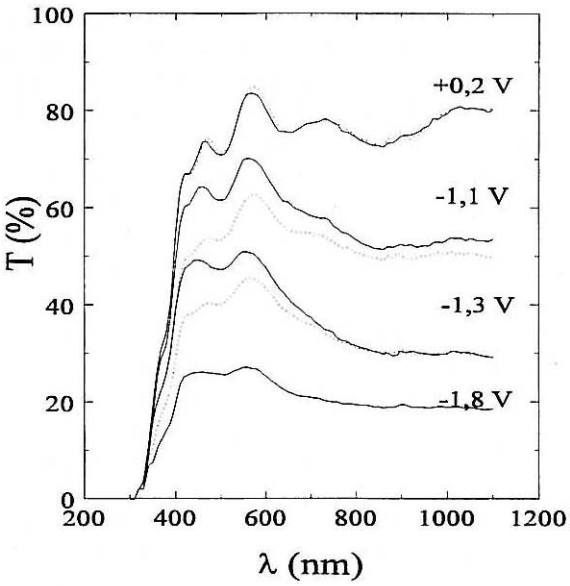

Fig. 8. Optical transmission spectrum of Nb_2O_5 thin film heat treated at 560 °C for 2 h in O_2 atmosphere and measured after different step potentials during a complete voltammetry cycle [68, 71–74]

chemical quality and stability appear quite adequate as substitute WO_3 coatings.

Ozer et al. [69] have also prepared Nb_2O_5 coatings by hydrolysis and polymerization reactions of polymeric niobium ethoxide solution in ethanol with addition of acetic acid. The films were prepared by a spin coating technique and then heat treated at 150 °C only, so that their structure was amorphous. The cathodic and anodic charge obtained at a sweep rate of 20 mV/s were approximately 20 mC/cm^2 for Li insertion and the films were found quite stable over 1000 cycles without significant change or degradation. As the films were amorphous their color was brown and the change in transmittance was only of the order of 30% in the visible range, with rather slow kinetics for coloring (30 s) but a fast rise time for bleaching (3 s). Such films are proposed as counter electrodes in anodically coloring EC nickel oxide devices.

4.3.6 CeO_2 and CeO_2 Doped with TiO_2 or SnO_2

CeO_2. Pure and doped CeO_2 coatings are promising materials to be used as optically passive counter electrodes (ion storage). This compound has two stable valencies available (III and IV) and is transparent in the spectral range 0.35–30 μm.

Only three works have been reported on their preparation. Atkinson and Guppy [139] prepared pure CeO_2 gel coatings from cerium hydroxide which were peptized with HNO_3 with a nitrate to ceria mole ratio of 27:100. However the authors only reported on the mechanical stability of the films in relation to crack formation. Recently Stangar et al. [40] have prepared pure CeO_2 sols by thermal decomposition of $Ce(NH_4)_2(NO_3)_6$. Peroxycomplexes were made by adding H_2O_2 to the yellow solution of the starting compound. A brown Ce(IV) complex decomposed into a yellow gelatinous precipitate which was used after peptization with HNO_3 for making very stable sols and homogeneous, crack free coatings with a particulate texture. The films heat treated at 520 °C are crystalline but exhibit a more amorphous structure when heat treated at 300 °C. The electrochemical properties show a high reversibility for Li^+ insertion (better then CeO_2–TiO_2, see below), stable after five cycles.

The total charge exchanged during cycling was found to be dependent on the thickness of the coatings and varied from 1 mC/cm^2 for a 25-nm thick film to 9 mC/cm^2 for a 250-nm thick coating (measured after 70 s). The interesting thing about these films is that they show only a coloration in the UV region typically below 370 nm (Fig. 9). It was claimed that their storage capacity was superior to CeO_2–TiO_2 coatings but their time response was inferior (see below).

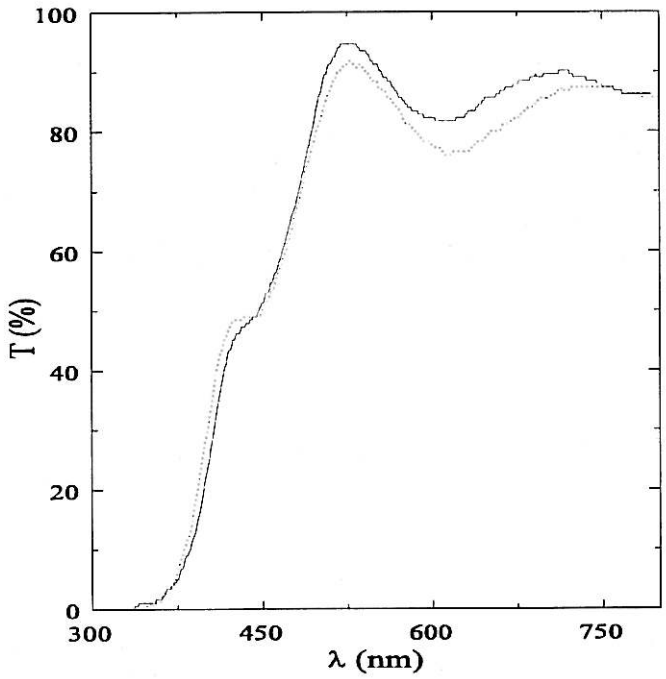

Fig. 9. Optical transmission of the system glass/ITO/CeO_2–TiO_2(sg) (——) before Li^+ insertion, (– – –) after Li^+ insertion [44, 46, 47]

Much better results have been reported by Orel and Orel [41] using sols made with the same precursor $Ce(NH_4)_2(NO_3)_6$. In this method precipates have been obtained by addition of NH_4OH at pH = 9. After washing with bidistilled water in order to remove NH_4^+, Cl^-, and NO_3^-, peptization was performed by adding an equimolar quantity of HNO_3 to obtain a colloidal sol. Coatings have been obtained by a dip coating technique followed by heat treatment at 300–500 °C. The authors report that the amount of charge exchanged increases with the CeO_2 oxide concentration in the sol and the thickness of the films (up to 8 dips corresponding to 280 nm). The highest value was about 20 mC/cm^2.

CeO_2–TiO_2. These compounds have similar (but better) electrochemical properties than pure CeO_2. Their preparation was first reported by Baudry et al. [43] and a series of other papers [44–48]. The sols have been prepared by dissolving cerium amonium nitrate, $Ce(NH_4)_2(NO_3)_6$, and titanium isopropoxide in ethanol, isopropanol or 2 methoxy-ethanol. The sol had to be aged for about seven days. In order to get the best electrochemical activity the dip coated film had to be fired at 450 °C. At this stage the structure of the films was essentially amorphous with the presence of small CeO_2 crystallites. Similar films obtained from sols prepared by mixing two alkoxides, $Ce(OBu^s)_4$ and $Ti(OBu^n)_4$, have later been reported by Kéomany et al. [49]. In this case the coating were found to be amorphous for concentrations of CeO_2 below 50% and the size of the CeO_2 nanocrystallites included in the TiO_2 amorphous matrix increases from $\sim$1 nm for 5% CeO_2 to 5 nm for pure CeO_2 [49]. Contrary to the work of Stangar et al. [40], the best electrochemical Li^+ insertion has been found for an equimolar mixed oxide [43, 49] with a total charge exchanged at 50 mV/min as high as 20 mC/cm^2 [49], almost a factor of two higher than that claimed by Macedo [50]. This is probably due to the fact that Kéomani et al. have prepared films with extremely small particles (or sites or hanging bond or defects structure which can receive the Li^+ ion), and the amorphous porous TiO_2 matrix probably appears as a more continuous structure for the Li^+ ions to reach the surface of each crystallite or site.

CeO_2–TiO_2 coatings have also been prepared by Stangar et al. [40] and Orel and Orel [41] using the route proposed by Makishima et al. [140] in which $CeCl_3$ was used in combination with titanium isopropoxide $Ti(OiPr)_4$ with a Ce/Ti mole ratio of one to one. Their overall properties were similar to those found by the Brazilian and French groups but their electrochemical properties were inferior. No comments about the CeO_2 nanoparticles have been reported.

CeO_2–SnO_2. Along the same direction Orel and Orel [41] have reported the preparation of SnO_2-doped CeO_2 coatings using sols made with $Ce(NH_4)_2(NO_3)_6$ and $SnCl_4$. The method of sol preparation is similar to that described above by the same authors for pure CeO_2. As before, those films are not colored in the visible region and significant improvement of charge transfer was obtained with films prepared with 17 mol% SnO_2, varying from 10 mC/cm^2 for a 60-nm thick film to 22 mC/cm^2 for a 280-nm thick film (eight coatings) to be

compared to 4 mC/cm^2 and 16 mC/cm^2 for pure CeO_2 coatings. However the charge capacity was found to decrease slightly with the number of cycles (up to 400). The total charge exchanged was also found to depend on the CeO_2 concentration in the sol. With a coating of eight films it typically varied from 13 mC/cm^2 for a concentration of 4.8×10^{-3} mol/20 ml to 20 mC/cm^2 for a concentration of 9.6×10^{-3} mol/20 ml.

All these sol-gel coatings prepared with doped CeO_2 now look very promising for use as a counter electrode for any EC all solid state devices. The possibility of controlling the various parameters at our disposition during the preparation of the sols or films has practically triplicated the amount of change since the original work of Baudry et al. [43].

4.3.7 Fe_2O_3 and Fe_2O_3 doped with TiO_2 or SiO_2

FeO_3. Only three recent works have been reported on the preparation and the characterization of iron oxide electrochromic coatings. Moser and Lynam [91] have used ferric nitrate-ethyl acetate solution and recently Orel et al. [92, 93] have precipitated $FeCl_3 . 6H_2O$ with $(NH_3)_{aq}$ followed by peptization of the precipitate with glacial acetic acid. Amorphous γ-Fe_2O_3 films obtained at 300 °C show electrochromic properties under Li^+ ions insertion (anodic coloration, $\Delta T = 60\%$ at 300 nm) but their transformation into α-Fe_2O_3 at 500 °C turns them inactive. The presence of OH^- in the coatings and small grain size particles were found of fundamental importance to develop electrochromism. The adherence of the films to the electronic ITO coating was poor and the mechanical stability deteriorated with cycling.

$Fe_2O_3 : TiO_2$ and $Fe_2O_3 : SiO_2$. The electrochemical stability of the iron oxide was modified by admixing (nonabsorbing Ti and Si oxides prepared with the $FeCl_3 \cdot 6H_2O$ precursor in combination with 3-aminopropylmethoxysilane (3-APMS) or ferric (III) nitrate alcohol solution in combination with $Ti(^iPr)_y$ respectively by Orel et al. [92, 93]. Mixed Fe/Ti and Fe/Si oxide films color and bleach in a narrower spectral range (300–400 nm) than pure Fe_2O_3 and the optical transmission variation drops to 15–30%. However the mixed oxides exhibit extremely large charge intercalation (up to 60 mC/cm^2), much higher than most of the known electrochromic coatings. This property makes these coatings interesting for use as counter electrodes (ion reservoir).

4.3.8 SnO_2

Olivi et al. [94] developed a new method for the synthesis of SnO_2 by using 50 wt% citric acid in ethylene glycol at 60 °C to which was added tin citrate in a 3/1 molar ratio (acid/tin) and a few drops of concentrated nitric acid in order to solubilize tin citrate and catalyze the esterification reaction performed at

110 °C. The films, calcined at 500 °C, are highly transparent in the 350–800 nm range, homogeneous and crystalline. No optical changes have been observed either in the oxidized or reduced forms using Li electrolyte. The charge associated with the process at a sweep rate of 10 mV/s was however very low, 4 $\mu C/cm^2$, but such a system also appears as an attractive material for transparent counter electrodes in transmissive EC devices using non-aqueous electrolytes.

4.4 Sol-Gel Conductive Coatings

Little work has been done on using the sol-gel process to obtain electronic and ionic conductive coatings with explicit functions for EC devices. In these systems the electronic conductors have the function of making electric contact between the external source and the device and should be able to insert and extract electrons from the EC coatings. However these coatings should also present a combination of optical, mechanical, chemical and aesthetic properties which have to be fulfilled at the same time. For instance, for EC devices used as energy saving windows, it is mandatory to have high IR reflection (9.5 μm), high transmission for solar and visible light energy and long term stability.

The electrolyte which is in direct contact with the EC layer (Fig. 3c,d) should exchange ions such H^+, Li^+, Na^+, etc. with it. Depending on the configuration of the device it may also serve as the ion storage (Fig. 3b, c) or unite the EC layer to the counter electrode (ion storage coating) and allow only the ions to migrate through it (Fig. 3d). To fabricate EC devices with good response times, the ionic conductivity should be higher than 10^{-7} S cm^{-1} and at least 10^{-4} S cm^{-1} for display devices.

4.4.1 Electronic Conductive Coatings

ITO. Several years ago Arfsten et al. [98, 99] developed sol-gel indium tin oxide (ITO) coatings prepared by dip coating with heat treatment between 400 and 500 °C in reduced atmosphere, to be used either alone as heat mirror coatings or in EC devices. The authors did not however disclose their preparation method but only their physical properties which are given in Table 5.

More recently Takahashi et al. [100] got similar results using a mixture of tin isopropoxide and indium acetate precursors stabilized with diethanolamine $(HOCH_2CH_2)_2NH$, or a mixture of indium alkoxide dissolved in isopropanol stabilized by triethanolamine to obtain In_2O_3 coatings and ITO coatings when adding Sn isopropoxide. This stabilizer was found to suppress the alkoxide hydrolysis leading to stable sols without the occurrence of gel formation and precipitation and to enhance the solubilities of alkoxides and even metallic acetates into alcoholic solvents.

Table 5. Optimized properties of ITO sol-gel for application in displays coatings with different thicknesses (a), (b), and (c) for windows

Properties	(a)	(b)	(c)
Film thickness (nm)	20–30	80–100	270
Density of carriers (10^{20} cm^{-3})	4	5–6	5–6
Mobility ($cm^2V^{-1}s^{-1}$)	15–20	60–70	35–40
Conductivity ($S\,cm^{-1}$)	800–1200	5000–6000	3000–3500
Sheet resistance ($\Omega\,cm^{-2}$)	500	~25	10

SnO_2. Sn(IV) oxide is a wide gap semiconductor (Eg = 3.97 eV) with transmittance cut-off at 335 nm. When doped with F, Sb or Mo it becomes electrically conductive while its optical solar transmission is invariant (85–95%). Due to the presence of free charge carriers introduced by doping, the films start to reflect thermal infrared radiation for $\nu > 2000\ cm^{-1}$. Because of these properties SnO_2 has a widespread use in various fields.

Different organic and inorganic precursors have been used for making SnO_2 powders and coatings via the sol-gel route. Up to now more studies have been devoted to the alkoxide route using Sn and Sb alkoxides [101–105, 107, 141]. Yet the drawback of the method is that alkoxides are expensive, extremely sensitive to heat, moisture and light and their preparation is time consuming.

The inorganic route relies on the mixing of soluble salts of Sn, such as $SnCl_4$ and $SnCl_5$, in combination with Sb salts such as $SbCl_3$ and $SbCl_5$. Gels of SnO_2 prepared entirely via the inorganic sol-gel route were reported by Goodman and Gregg [108]. Undoped SnO_2 gels were also made by Giesekke et al. [109] and recently by Hiratsuka et al. [106] who succeeded in decreasing the time for gelling the sols by peptizing the precipitates with NH_4^+ and OH^- ions. They also found that an excess of Cl^- ions retarded the gelling time. SnO_2–Sb_2O_5 semiconducting glaze [111] was also made from $SnCl_4$ and $SbCl_5$ precursors, using H_2O_2 in combination with an alcohol as solvent for the preparation of Sn-based gels.

Maddalena et al. [107] reported electrically conductive Zr- and Ti-doped SnO_2 films prepared from the $SnCl_2$ precursor in combination with $Zr(OC_3H_7)_4$ and $Ti(OC_4H_9)_4$. The alcoholic solution of the precursor underwent gelation when left in an open vessel for 5 days at 30 °C.

Orel et al. [110] have prepared an undoped SnO_2 thin solid coating by dip-coating techniques using an aqueous $SnCl_4$. $5H_2O$ precursor peptized with $(NH_3)_{aq}$. Sn-doped coatings have been achieved by adding $SbCl_3$ to the sol in concentrations of 1–10 mol%. Analysing the plasma frequency determined by FTIR reflection spectroscopy, they reported that the concentrations of free carriers in their sample were smaller compared to those obtained with SnO_2 prepared by spray pyrolysis or RF sputtering, despite the large concentration (10%) of the dopant species introduced. The films have a visible near infrared transmittance of about 75% and exhibit, when measured without post heat treatments, (i.e. as deposited), a conductivity of about $83\ S\,cm^{-1}$. However it

decreases with the film thickness because the crystallization is favored at greater coating thicknesses. The dip coating process could be repeated up to 20 times.

V_2O_5. V_2O_5 films have also been proposed as conductive coatings. Pozarnsky et al. [112] have obtained thin films from sols prepared by ion-exchange of sodium metavanadate solution. They found that their thickness and surface morphology were directly related to the age of the sol. The last property was found to change from that of a featureless surface after one day to a continual coverage of micron-sized fibers as the sols aged. The conductivity of the coating, which is of the order of 2 to $3 \times 10^{-4}\,S\,cm^{-1}$, was unaffected by the aging process.

4.4.2 Ionic Conductive Coatings

An ionic conductor is an electrolyte which is able to conduct ions such H^+, Li^+, Na^+, K^+, etc. In EC devices H^+ and Li^+ are most used as they have a higher mobility and Li^+ ionic conductors are preferred because of their low corrosive effect at the adjacent coatings. For most EC devices the electrolyte must be transparent and preferentially of solid state to avoid any leakage or pressure gradient observed with liquid ones. Although the literature on ion conductors is vast (several reviews on inorganic ion conductors suitable for EC devices and other applications can be found in [7] and [86]), only a few works have been produced on sol-gel process and the description of their properties in EC devices is rare. In fact, to date, all commercial devices use liquid or polymer type electrolytes. This is essentially due to their position in the EC devices (Fig. 3) which makes fabrication of all solid state devices rather difficult, as the chemistry and heat treatments required to place one more solid state layer and maintain the interface and the structure of the underlying layers (EC electronic conductor/glass and storage coating/electronic conductor/glass) become rather restrictive. In addition one would have generally to charge one of the electrodes with the ions before completing the stack and ensure that the nature of the bonds between these ions and the matrix is not altered or the ions do not migrate during further processing. A major limitation with the sol-gel process, which has been observed and yet not overcome, is the inability to produce a material that can solidify without releasing volatiles or that does not change either through aging or during the cycling process over long periods of time. Usually reactions, such hydrolysis and condensation, continue after device assembly and separate the interfaces with the formation of bubbles.

According to Grandqvist [142] the requirements for such coatings should be:

(i) high ionic conductivity, between 10^{-4}–10^{-7} S/cm depending of the application;

(ii) electronic conductivity smaller than 10^{-12} S/cm;
(iii) long cycling durability at operation temperature;
(iv) good adhesion with the adjacent layers and optical transparency in the spectral range of interest.

Most of the research in this field has been realized in order to obtain sol-gel conductive coatings for H^+ and Li^+ to which we shall restrict our discussion. In both cases there are basically two classes of materials which may serve for this purpose. The first one is based on the fabrication of inorganic oxide material and the other, more promising from our point of view, on the preparation of organic-inorganic hybrids which combine the better conductive properties of polymer type material with the better mechanical strength of inorganic backbone. Also, from the point of view of the fabrication of complete devices, the Ormocer type coating will be easier to use. However to our knowledge none of these coatings are presently employed in commercial products which are all built with liquid electrolytes.

H^+ Conductor. The only inorganic H^+ conductor coating which has been described for such applications is Ta_2O_5. Ling et al. [116] have reported the preparation of spin-coated Ta_2O_5 thin films, pure or doped with Al, using the alkoxide route (Ta ethoxide). The films have been studied with heat treatment up to 1200 °C. As their goal was to improve the storage of dielectric capacitor, they did not report any conductivity data.

Recently Ozer et al. [117] have prepared Ta_2O_5 from the same route using a mixture of tantalum ethoxide ($Ta(OC_2H_5)_5$) , acetic acid and water. Spin coated films at 2500 rpm on ITO glass or ITO coated with WO_3 on glass have then been heat treated at 150 °C for 1 h. The preparation of thick films required 10–15 repetitions of the above procedures, and the films were found to be hard, durable and stable. From a.c. impedance and electrochemical measurements, the authors conclude that the sol-gel films have higher ionic conductivity and better properties than Ta_2O_5 films obtained by other methods. Depending on the deposition conditions, ionic conductivities as high as 5×10^{-6} S cm^{-1} have been obtained, i.e. almost a factor two higher than RF sputtered films. This increase in conductivity is thought to come from the fact that the sol-gel films are more porous (packing density $\rho = 3.2$ g/cm^3) than the films deposited by other techniques, thus providing a larger surface area for absorbing the protons. Tests performed on half an EC window glass/ITO/WO_3/Ta_2O_5 (190-nm thick) with a H_2SO_4pH = 2 solution as electrolyte resulted in strong transmission variation between the colored and bleached states. The photopic weighted change and the solar weighted transmittance change are $T_p = 85.1\%$–21.9% and $T_s = 75.6\%$–14.2% respectively. The voltammograms do not present degradation up to 150 cycles.

Charbouillot et al. [120] were the first to propose a promising new family of advanced materials which they called AMINOSILS. These compounds were prepared by hydrolysis and condensation of organo-tri-alkoxide-silane

$R'Si(OR)_3$ (R' = amino group) in presence of a strong mineral acid – $HClO_4$, HCF_3SO_3, HCH_3SO_3, HCl, HNO_3, HCH_3COO or H_3PO_4, and water. The silica backbone provides mechanical strength while the organo amino groups offer solvation properties with respect to guest ionic species. Non-porous films about 10 μm thick were found to be stable in atmospheric atmosphere and up to 180 °C. At room temperature their conductivity is about 10^{-5} S cm^{-1}.

At the same time Judeinstein et al. [121] have proposed an organic modified TiO_2 gel made from a sol prepared from a mixture of acetic acid and pure $Ti(OBu^n)_4$ to which was added glycerol ($CH_2OHCH–OHCH_2OH$) in a molar ratio glycerol/Ti ranging between 12 and 30 to 1. During the reaction it is believed that the metal alkoxide reacted with the glycerol forming organic bridges between Ti atoms. The hydrolysis of the alkoxy group was performed in excess water. The resulting viscous gel was stable up to 80 °C. The conductivity was deduced from the intercept of the arc of a circle with the real axis of the a.c. electrical impedance plotted in the complex plane and was found to follow an Arrhenius behavior $\sigma T = \sigma_0 \exp(-Eg/kT)$ in the temperature range -40 to $+60$ °C. Room temperature conductivity varied between 3×10^{-6} and $10^{-5}\ \Omega^{-1}\,cm^{-1}$. It increases with the amount of acetic acid while the activation energy increases with the amount of glycerol. This coating was tested with satisfactory results in a complete sol-gel EC window (see Sect. 4.5).

A new proton-conducting polymer electrolyte, poly (benzylsulfonic acid) siloxane (PBSS) was developed by a sol-gel process by Sanchez et al. [122]. The hydrolysis and condensation reactions of triethoxybenzylsilane were studied under different catalytic conditions. PBSS was found to be thermally stable up to 300 °C in air and high conductivities ranging from 2×10^{-3} to 10^{-2} S cm^{-1} at room temperature were measured by a.c. impedance spectroscopy. The same laboratory [143] had also previously developed a proton-conducting polymer based on the copolymerization via the sol-gel process of sulfonamide-containing groups partially deprotonated and an internal plasticizer (polyethylene oxide (I) segments). All the organic groups are attached to trialkoxysilanes which act as the silica-based backbone. The films were found to be flexible, homogeneous, transparent, thermally stable up to 220 °C and electrochemically stable up to 2 V. The highest conductivities, 2×10^{-7} S cm^{-1} at 30 °C and 10^{-5} S cm^{-1} at ~84 °C, have been obtained with ~15% sulfonamide deprotonated groups and ~10% of (I) plasticizer (weight average molecular weight 2000).

Another interesting approach, discussed earlier (Sect. 4.3.3), has been reported by Stangar et al. [59] who developed a combined electrochromic ion conductor based on phosphotungstic acid (PWA) doped TiO_2 gels, which already contained protons. Using a.c. impedance spectroscopy the authors found that, at room temperature, PWA/Ti gels have a higher proton conductivity ($\sigma = 1.7 \times 10^{-4}$ S cm^{-1}) than pure TiO_2 gels ($\sigma = 4.6 \times 10^{-6}$ S cm^{-1}) or even aminosils [120]. Higher values ($\sigma = 10^{-2}$ S cm^{-1}) were found with PWA/Si gels by Tatsumisago et al. [144] and for water soluble PWA doped polyvinyl alcohol (PA) gels (σ up to 9.8×10^{-2} S cm^{-1}).

Stangar et al. [59] have also prepared silica gel from 3-aminopropyl-triethoxysilane with R = HPA/Si = 0.1. Their conductivity was about 2.2×10^{-5} S cm^{-1}, higher than that of aminosils doped with acid having small ions. The authors claimed that the small polarizability of the large Keggin's ion decreases the influence of ion-ion interactions leading to an increase in proton conductivities.

Li^+ conductor. Lithium ion conducting amorphous solid state inorganic materials such as glasses and glass ceramics are materials to be considered for solid state batteries and related EC devices. They exhibit isotropic ionic conductivity but their preparation by conventional melting techniques requires high temperatures which limits the alkali concentration. Therefore the preparation of fast ion Li or Na conductors by the sol-gel process is certainly an asset. This field has recently been reviewed by Boilot and Colomban [145], Klein et al. [146] and Klein [147].

Earlier works on these materials essentially concentrated on the preparation process itself. It was found that the lithium gels were more stable than their sodium and potassium counter-parts and that the glasses and glass-ceramics derived from lithium silicate gels are more stable and more durable in corrosion tests. Among the different compositions studied, the family of sodium zirconium-silico-phosphate gels known as Nasicon (Na Super Ionic Conductor) has been prepared from a mixture of alkoxides [145], and room temperature conductivities as high as 10^{-6} S cm^{-1} for gels and up to about 10^{-3} S cm^{-1} for glasses have been achieved. In the last case the conductivity was found to be similar to those of equivalent polycrystalline ceramics with, however, a higher activation energy.

More promising results seem to have been obtained in systems containing other network formers such as P_2O_5 [148–150], Al_2O_3 [151], Ga_2O_3 [152] and V_2O_5 [153].

Hayri and Greenblatt [148, 154] have studied the fabrication of Li_2O (Na_2O)-SiO_2–P_2O_5 xerogels and found that the conductivity increases with the concentrations of both lithium and phosphorus, obtaining relatively high values up to 2×10^{-3} S cm^{-1} at 300 K. However the conductivity was found to be associated with protons which always exist in different forms in xerogels (surface hydroxyls, hydrogen bonded water, etc.) as the process is carried out in aqueous media. Nevertheless several studies have been performed on these systems in order to understand their chemistry, molecular structure and microstructure (see [147] for references).

Wang et al. [151, 152, 155–157] have studied the ionic conductivities of $(LiCl)_2$–R_2O_3–SiO_2 with R = B, Al, Ga xerogels. The materials have been prepared by mixing a solution of TEOS dissolved in methanol with a solution of aluminium nitrate dissolved in methanol to which was added acid and water and then LiCl. Dip coated films ~0.8 μm thick have been dried and then heat treated at 300 °C. XPS measurements indicate the presence of residual organics with possible atmospheric carbon contamination and show that the oxygen has

three forms: bridging (BO), non-bridging (NBO) and O = C–O–. The highest lithium conductivity (measured by a.c. impedance) was found in the lithium alumino silicate xerogels and was attributed to the relatively large concentration of mobile lithium ions associated with tetrahedral AlO_4 units and/or with non-bridging oxygens in the silica network [151]. Linear behavior was observed in the temperature range from 100 to around ~300 °C. The presence of organics or carbon residues is claimed to have an insignificant effect on the ionic conductivity. At temperatures below 100 °C, σ is lower than 10^{-7} S cm^{-1}, with an activation energy of 0.75 eV, a value which is much lower than that of polymers and which is not acceptable for the fabrication of EC devices. However these films have the advantages of a better stability at higher temperature and good mechanical strength.

Solid state batteries of the type Ni/oxide cathode (Li_yMnO_2)/lithium aluminosilicate gel/Li/Ni have recently been realized [158], having initial open circuit voltages up to 3.4 V.

In lithium silicate gels, a.c. conductivity is determined by the pore size and density, the water content and the precursor salt in terms of the anion. At room temperature its value is low, of the order of 10^{-7} S cm^{-1} but increases with temperature according to an Arrhenius law (as the process is thermally activated).

V_2O_5 has also been tested by Trifonova [159] to be used as an electrode material for solid state rechargeable lithium batteries. The sol was made using a decavanic acid solution prepared by passing a 0.25 mol/l sodium vanadate solution through a cation (H^+) exchanger in order to eliminate completely the Na ions. The sol polymerized spontaneously on standing. The gel was spread manually on Ni foil and dried. Composite electrodes of $V_2O_5 \cdot nH_2O$ and PEO were also prepared to improve the mechanical properties of the films. The electrochemical characterization was performed in an all solid state cell with a polymer as electrolyte Li/PEO–$LiCF_3SO_3$/$Li_xV_2O_5 \cdot nH_2O$. The maximum energy density was 460 Wh/Kg obtained for $Li_{1.35}$ V_2 $O_5 \cdot 0.5nH_2O$, a modest value, and the cycling was found to be fully reversible only if all the loosely bound water is eliminated by heat treatment (dry gels). Up to now none of the inorganic systems have been used for EC devices.

The most promising low temperature Li^+ ion conductors materials seem to be lithium doped ORMOCER. In a recent study ORMOLYTES (ORganically MOdified electroLYTES) have been prepared and characterized by diverse techniques by Judeinstein et al. [160] from mixtures of tetraethoxysilane, tetraethylene glycol (PEG_n) and lithium salt ($LIC1O_4$) . Transparent monoliths and films have been obtained. Their structure was found to be diphasic with silica clusters (observed by SAXS) providing the mechanical properties and with an organic phase allowing the dissolution of large quantities of salt. Their thermal stability was checked between − 25 and + 95 °C. The values of the ionic conductivity measured at 300 K in anhydrous materials treated in vacuum and after heat treatment increased drastically with the amount of lithium salt and varied between 10^{-8} and 6×10^{-5} S cm^{-1}, much larger than that of the

pure matrix ($< 10^{-10}$ S cm^{-1}), proving that the conductivity came from the dissolved salt. As a function of temperature, deviation from an Arrhenius law has been observed revealing two different slopes and the activation energies were found to be between 0.5 and 0.9 eV.

In earlier work, Judeinstein et al. [121] incorporated $LiClO_4$ in the modified hybrid TiO_2 gel. This material, which is already a good proton conductor, exhibits even higher conductivity with lithium ions, up to 4×10^{-4} S cm^{-1} at room temperature. The process is also thermally activated (E = 0.45 eV).

4.5 Sol-Gel Electrochemical Devices

A few groups have developed EC devices in which either some or all active layers have been prepared from gels. The first windows were reported by Judeinstein et al. [121] for which both the EC layer and the electrolyte were made from gels. They had the following configuration: non-symmetric SnO_2/WO_3(sg)/TiO_2–$LiClO_4$(sg)/SnO_2 or symmetric always colored SnO_2/WO_3(sg)/TiO_2–$LiClO_4$(sg)/WO_3(sg)/SnO_2. The non-symmetric window was initially transparent. The main characteristics are given in Table 6.

Various small size windows have been mounted in Aegerter's Advanced Materials Laboratory to test some of the sol-gel coatings made there. The CeO_2–TiO_2 storage layer was tested in a cell ITO/Li_xWO_3 (evaporation)/POE–$LiN(CF_3SO_2)_2$/CeO_2–TiO_2(sg)/ITO showing a transmission from 60 to about 20% (at 750 nm) and reasonable kinetics, limited by the insertion process of Li^+ into the CeO_2–TiO_2 layer [45, 48, 50] (Fig. 10). Similar results have been obtained substituting the polymer electrolyte by a cellulose polyacetate polymer, a proton conductor. Its kinetics were faster but the window lifetime was shorter due to corrosion problems at the WO_3 coating by the acid (protonic) conductor [46, 50, 161]. Sol-gel TiO_2 protonic conductors similar to that proposed by Judeinstein et al. [121] have been tested in symmetric and non-symmetric windows of configuration [44, 47, 50]:

1) ITO/CeO_2–TiO_2(sg)/TiO_2(sg)/CeO_2–TiO_2(sg)/ITO;
2) ITO/H_xWO_3(sg)/TiO_2(sg)/CeO_2TiO_2(sg)/ITO;
3) ITO/H_xWO_3(evap.)/TiO_2(sg)/CeO_2–TiO_2(sg)/ITO.

The first window does not present any coloration (see Sect. 4.3.6) and no degradation has been observed up to 30×10^3 voltammetry cycles. The optical transmission of the second one can be seen in the first and 360th cycles (Fig. 11) where the effect of the corrosion at the WO_3(sg)/TiO_2(sg) interface is clearly observed. During the first cycles the performance of the windows was found to be similar to those made by conventional processes. Better results should however be obtained by using Ti butoxide instead of Ti isopropoxide for the preparation of the electrolyte with rigid control of the amount of water in the preparation of the WO_3 (sg) layer.

Table 6. Characteristic of all-gel electrochromic cells (6 cm^2) corresponding to a change in optical density of 0.8 [121]

	Non-symmetric	Symmetric
Coloration voltage	− 3.5 V	− 2.5 V
Response time	50 s	50 s
Bleaching voltage	+ 2.0 V	+ 2.5 V
Response time	50 s	50 s
Lifetime (cycles)	$> 3 \times 10^3$	$< 4 \times 10^4$
Open circuit Memory	4 months	> 6 months many months

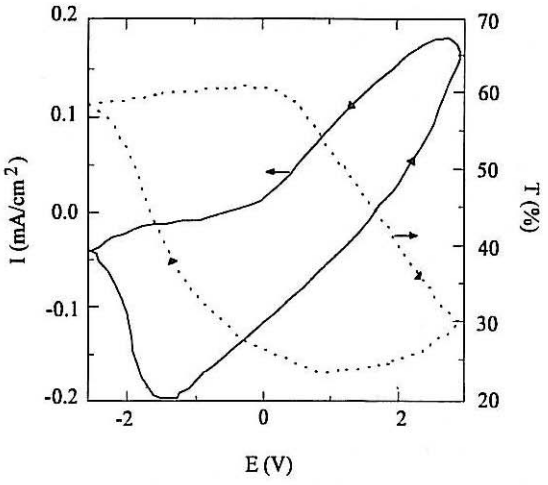

Fig. 10. Opto-electronic cyclic voltammetry of an EC window ITO/Li_xWO_3(evap)/POE-LiN$(CF_3SO_2)_2$/CeO_2-TiO_2(sg)/ITO measured at $\lambda = 750$ nm [45, 48, 50]

Ozer et al. [56] have built an "all-gel" device with the configuration ITO(sg)/TiO_2(sg)/electrolyte(gel)/ITO(sg) in which the electrolyte was a gel prepared from poly (vinylbutyral), glycol ether and LiCl. The response time was ~50 s under applied voltage of ± 2.8 V with open circuit memory as long as 5 months.

The performance of a transmissive EC device with the configuration ITO/WO_3/H_3PO_4-polyvinyl alcohol (PVA)/SnO_2:Sb(sg), where the last layer acts as an ion storage and conductive electrode, has been briefly reported by Orel and Orel [41], who reported large optical transmission variations mainly in the near-infrared region. The coloration kinetics were adequate but the bleaching kinetics lasted from 1 to 3 min.

Stangar et al. [59] have also tested a thin PWA/Ti xerogel film in a semi-liquid electrochromic EC cell with reflectance modulation. The gel was found to change color irreversibly from transparent yellow to blue. Reversibility was achieved by putting a thin Ag film acting as a counter electrode in contact with

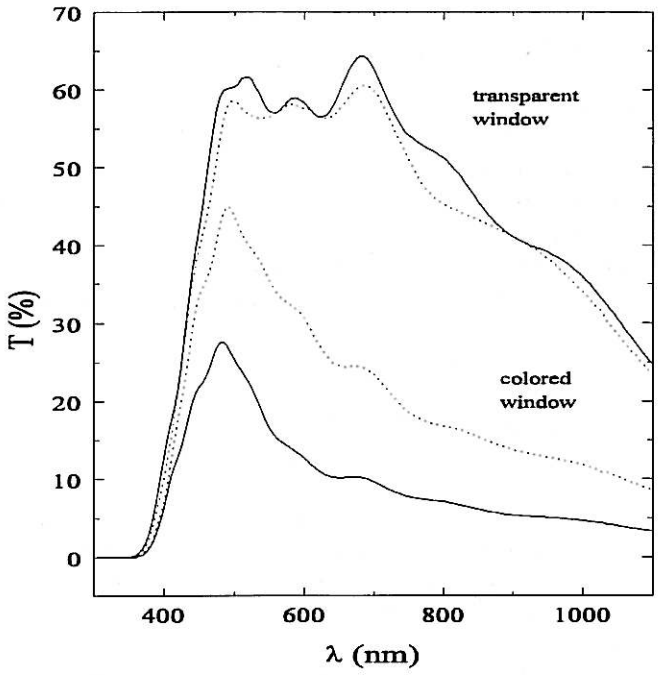

Fig. 11. Optical transmission of an EC window ITO/H_xWO_3(sg)/TiO_2(sg)/CeO_2–TiO_2(sg)/ITO measured during the first cycle (——) and the 360th cycle (– – – –) [44, 47, 50]

one of the ITO electrodes. The electrochromism behavior of PWA/Ti solid films was verified in an all solid state device ITO/PWA:Ti(sg)/H_3PO_4–PVA/SnO_2:Sb(sg). Reversible response was reported with well defined anodic and cathodic peaks. However the transmittance changes were smaller than 15% due to the small thickness (200 nm) of the PWA/Ti EC film into which only 4 mC/cm^2 could be inserted. The reversibility and cyclability were claimed to be satisfactory.

Other systems involving at least one sol-gel layer can be found in [162, 163]. Developments are also being made in different industrial laboratories but no public disclosures are yet available.

The fabrication of all solid state EC devices is quite a difficult task. Nevertheless several sol-gel films have been shown to have adequate properties to be used for such a purpose. CeO_2–TiO_2 layer (which was also prepared recently using conventional techniques) looks promising as a storage coating but its charge capacity should be slightly improved. Nb_2O_5 is a promising EC layer but WO_3 coating is today the best candidate from the scientific and technological points of view and recent results indicate that it will be used soon for EC rear-view mirrors in automobiles. The main challenge remains the development of an adequate Li^+ solid state electrolyte. With our present knowledge inorganic

glasses or glass-ceramics still have too low ionic conductivity and cannot be used in EC devices which have to tolerate temperatures as low as $\sim -20\,°C$. They can be useful for other applications such as high temperature batteries. The best systems to be contemplated are hybrid organic-inorganic materials (ORMOCER, ORMOSIL or ORMOLYTES). The results obtained up to now are promising but need to be improved. Another important problem which is rarely mentioned is the physical and chemical compatibility of these different materials at their interface and research is needed in this direction, bearing in mind parameters such as long term corrosion and cyclic durability and the large temperature variation to which EC devices will be submitted (-20 to $100\,°C$).

5 Materials for other Chromogenic Devices

As mentioned in the introduction, besides electrochromic materials, other materials present chromogenic properties which can be used to develop devices for optical transmission modulation with regards to luminous and solar radiation. The sol-gel researches in the field of *photochromism, thermochromism and electrooptics* are relatively recent and the sol-gel method looks very promising and particularly well adapted to incorporate molecules or nanoscale crystallites in an inorganic or mixed inorganic-organic matrix which can change their optical properties by light irradiation, temperature variation or application of an electric field respectively.

5.1 Sol-Gel Photochromic Materials

The feasibility of incorporating a photochromic dye (Aberchrome 670) into SiO_2 gels was first reported by Kaufman et al. in 1986 [164]. Later Levy et al. [165, 166] introduced spiropyrane molecules in silica matrices and studied their photochromic behavior during the transition sol $\rightarrow$ xerogel, showing the importance of the local environment near the molecules on such properties and the effect of the precursor materials used for the preparation of the sols. Analogous results have been obtained by Matsui et al. [167]. Photochromism of spiropyranes has also been investigated in aluminosilicate gels derived from diisobutoxy-aluminoxy-triethoxysilane by Preston et al. [168]. No reverse photochromism was observed and both the photochromic response and the color change rate decreased during the drying process, ceasing after a weight loss of around 75%.

Nogami and Sugiura [169] have studied the effect of the Al_2O_3 content of spiropyrane molecules in Al_2O_3–SiO_2 prepared from alkoxide precursor and found that the photochromism response decreased with increasing Al_2O_3 content. No more response was observed for 33% Al_2O_3.

More recently Yamamaka et al. [170] incorporated 2,3-diphenylindenone oxide (DPIO) into aluminosilicate, silica (TMOS) and ormosil sols prior to gelation. After gelation these materials are colorless. Upon exposure to ultraviolet light the organic molecule isomerizes to form 1,3-diphenyl-2-benzopyrilium-4-oxide (DPBO) and the materials turn red. The interconversion back to the colorless state was facilitated by exposing the molecule to visible light of wavelength greater than 435 nm. The fading of the absorption after blocking the UV irradiation is characterized by long lifetime components ($\sim$20 s) in all three types of materials but in addition, a short one ($\sim$5 μs) was found in aluminosilicate samples. All matrices showed a gradual decrease in their lifetime with time (measured up to 120 days after the gel preparation) which, according to the authors, may result from the increase of the polarity in the gel environment during aging.

Photo isomerization of 4-methoxy-4'-(2-hydroyethoxy) azobenzene (MHAB) in SiO_2 gel films was investigated by Ueda et al. [171] and their results have been compared with those obtained using the same dye incorpored in poly(methylmetacrylate) (PMMA) films. The cisfraction in the photostationary state in the sol-gel films was smaller than in PPMA films due to the higher rigidity of the sol-gel matrix. Later Ueda [172] reported on the effects of the introduction of one or two trimethoxysilyl groups (TES) into the AB molecules on the photochromism. The introduction of one TES group has only a slight influence on the photoisomerization and thermal reversion, but the incorporation of two TES groups depressed these parameters in the sol-gel films.

Spirooxazine molecules (SO) were also incorporated in ORMOCER by Hou et al. [173], prepared from organically modified silicon alkoxides $R'Si(OR)_3$ such as methyltrimethoxysilane (MTMS), and 3-glycidyloxypropyltrimethoxysilane (GPTMS) which have longer GP chains to create more flexible matrix for the dye and give additional polymerization between the epoxy groups. However the gelling time of these compounds is too long (> 1 month). When mixed together these precursors produced an interesting matrix which possesses thermal and photochemical stabilities comparable to SO-doped PMMA material with, however, much better photochromic response and faster color-change rate. However the fast decrease of the light induced absorption with temperature (up to 35 °C) still remains a problem.

Hou et al. [174] have also introduced photochromic dyes in aluminosilicate gels and monitored their photochromic properties during the sol-wetgel-xerogel transformation. The photochromic activity of the aluminosilicate gels decreases rapidly and even vanishes in the wetgel-xerogel stage while that of ORMOCER was found to level off at a reasonably high photochromic intensity which remains almost unchanged for over 4 months. The color-fading speed was, however, found to be similar to that in ethanol but the photostability was considerably improved.

Along the same direction, Judeinstein [175] has initiated research using polyoxymetallates (POM) as precursors prepared by reacting trichloro (or trialkoxy) silane with lacunar $K_4SiW_{11}O_{39}$. The POM are small compact oxide

networks about 1 nm size based on the sharing of MO_6 structural unit (M = W, Mo, V...) with a very high electronic density and interesting redox properties. The final material has been modified by adding radical such as vinyl, allyl, styryl, methacryl which have then been linked together via radical polymerization or by hydrosilation reactions between silane and vinyl derivatives or direct reaction of POM with bis (trichlorosilyl) derivatives. Transparent films of 0.3–1 μm thickness have been deposited. They turn blue upon UV irradiation or electrochemical reduction due to the occurrence of a wide absorption band in the visible-IR range characteristic of an intervalence transition W^{5+}–W^{6+} of the polymetallate.

It appears therefore that the synthesis of mixed organic-inorganic materials with a mixing of the components at the molecular scale leads to a great flexibility to reach materials with improved specific properties for all kinds of chromogenic applications and also for catalysis. These advanced compounds, nanocomposites or dye incorporated ORMOCER, open a brand new field with promising prospects.

Finally, to our knowledge, only one piece of work has been successfully carried out with inorganic photochromic materials. Photochromic glass coatings 1.5 μm thick were synthesized by Mennig et al. [176] by infiltration of Ag^+ into a predried Na–Al–B–Si gel layer. The formation of small Ag colloids was initiated by a soft heat treatment and then converted to AgCl crystallites of about 40 nm diameter by a HCl vapor treatment. Such coatings turn brown-violet under Hg-Xe light or Ar laser irradiation due to the formation of Ag crystallites of about 5 nm. The reverse process was realized by heating at 400 °C. It is claimed that no decay was observed after numerous cycles. Holograms have been obtained.

5.2 Sol-Gel Thermochromic Materials

Although several transition metal oxides or sulfides are known to undergo a sudden metal-to-nonmetal transition over a discrete temperature range [177] with pronounced and reversible changes in the optical (thermochromism), electrical conductivity and magnetic properties, very few works have been reported on the sol-gel preparation of such materials and the characterization of such properties.

Vanadium dioxide, VO_2, is known to undergo such a thermally induced semiconductor-to-metal phase transition at 68 °C [177]. Early works of Geffcken and Berger [178] and Schroeder [179, 180] are now being revived as today the state-of-the-art of the sol-gel process offers distinct advantages over the vacuum deposition of thin metal oxide films. Potember and Speck [181] have synthesized VO_2 film from a sol prepared from $V(Ot\text{-}Bu)_4$ dissolved in isopropanol to which was added W and Mo impurities in the form of oxytetraethoxide in order to modify the transition temperature. After hydrolysis and condensation under N_2 atmosphere, glass slides were dip coated and heat

treated at 600 °C under N_2 to prevent the oxidation of the vanadium compound. The product formed is $V_{1-x}M_xO_2$ and the reduction of VO_2 was performed in 1 mTorr vacuum at 600 °C (or in nitrogen atmosphere). Figure 12 shows the spectral transmission of a 100 nm thick VO_2 film above and below the transition temperature and Fig. 13 shows the temperature dependence of the optical

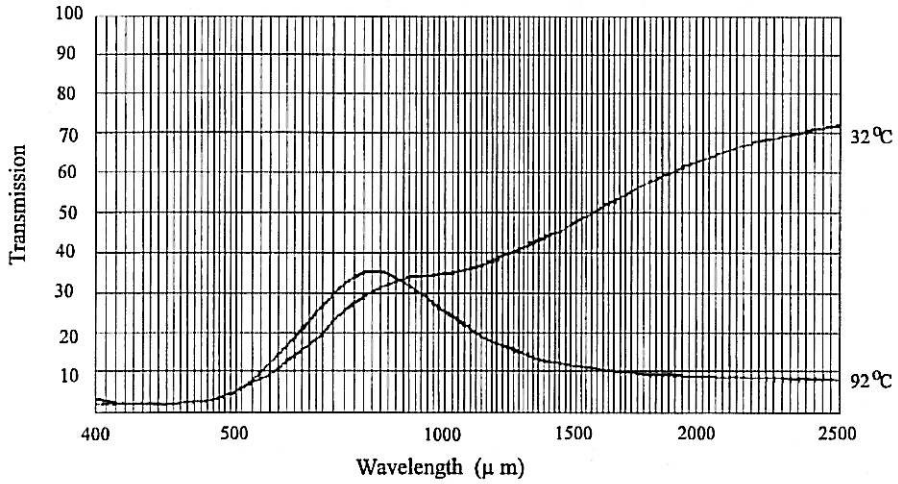

Fig. 12. Spectral transmission of a 100 nm thick sol-gel VO_2 film above and below the transition temperature [181]

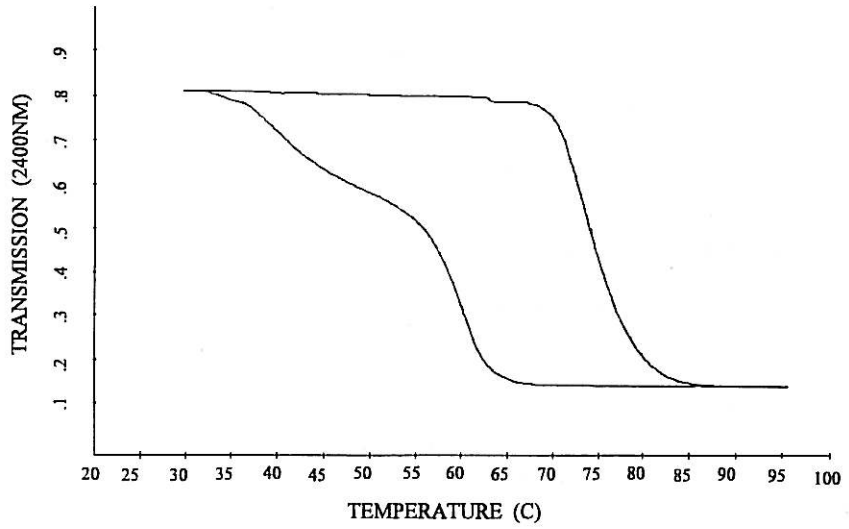

Fig. 13. Temperature dependence of the optical transmission of the same film at 2.4 μm, showing hysteresis effect (the transmission T increases at a temperature 10 °C lower on cooling) [181]

transmission at 2.4 μm. Stoichiometry, film thickness, type of substrate and crystalline orientation were found to affect the thermochromic properties.

5.3 Sol-Gel Electrooptical Materials

Electrooptical effects have been demonstrated by Levy's group [182 –186] by trapping dispersed microdroplets of liquid crystals (LC) in silica gel-glass (GDLC).

A mixture of methyltriacethoxysilane, K15 (4'-pentyl-4-biphenylcarbonitrite) and bidistilled water was polymerized at room temperature. The addition of Ti isopropoxide has also been used as dopant to increase the gel-glass refractive index and to reduce the refractive index differences between LC and matrix. This new class of doped sol-gel materials was sandwiched between two glass plates coated with transparent conductive electrodes. The device shows a reversible switching from opaque to clear transparent state when a voltage is applied to the conductive electrodes and acts as an optical shutter which, unlike other LC

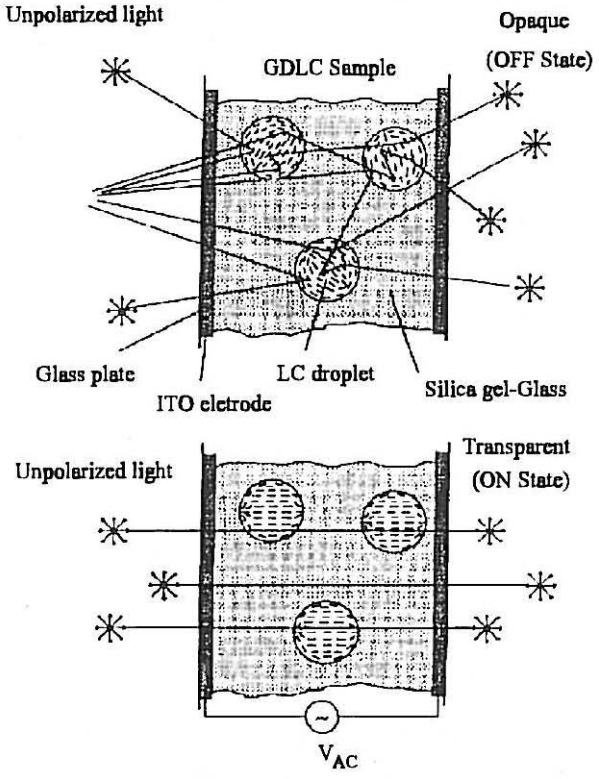

Fig. 14. Illustration of the switching principle of a GDLC device [184]

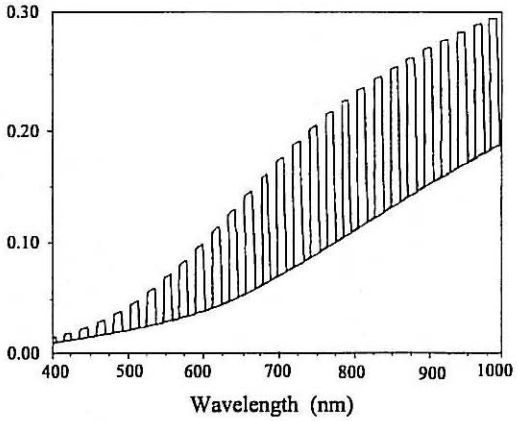

Fig. 15. Transmission spectra of a doped 30 μm thick GDLC (1:57 TIPO, 3.4:1 ethanol molar ratios relative to silane), switching peak voltage 150 V (saturation) [184]

devices, does not require polarizers. The optical switching is based on the dielectric anisotropy and birefringence of LCs where the applied electric field produces a torque that reorients the LC molecules, modifying in turn the refractive index encountered by the incoming light. Figure 14 illustrates the switching effect of such a device and Fig. 15 shows a typical spectral change of optical transmission. The dynamic behavior of such a device (typically in the range of 1 to 10 ms) was found to depend on the size of the LC droplets.

6 Sol-Gel Materials for Solar Cells

The sol-gel process can produce nanometer sized particles of several oxides [103] which can be deposited on a conducting glass support leading to transparent nanocrystalline films. When the materials have semiconducting properties (TiO_2, Fe_2O_3, Nb_2O_5, etc.) they should find a variety of interesting applications based on the fact that very large internal surface areas, with roughness factors of the order of 1000, are easily obtained. If the particles are sintered together to allow electronic contact, they can allow for electronic charge carrier conduction. A first practical embodiment uses such films for conversion of light to electricity (solar cell) which, in contrast to a conventional photovoltaic cell, separates the function of light absorption and carrier transport. The light harvesting is carried out by a sensitizer coated on the surface of the particles which initiates electron transfer events in the semiconducting particles leading to charge separation. The principle of the device, originally developed by Graetzel several years ago (a review can be found in [187]) is shown in Fig. 16.

When derivatized with suitable chromophore such as ruthenium complexes where one of the ligands is 4,4′-dicarboxy-2,2′-bipyridyl, Graetzel [188] has

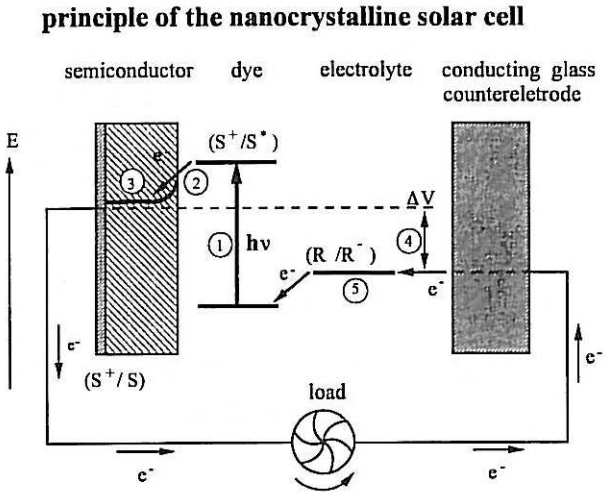

Fig. 16. Schematic representation of the principle of new photovoltaic cell indicating the electron energy level in the different phases. The cell voltage observed under illumination corresponds to the difference in the quasi-Fermi level of TiO_2 under illumination and the electrochemical potential of the electrolyte. The latter is equal to the Nernst potential of the redox couple (R/R^-) used to mediate charge transfer between the electrodes. The *layer 3*, 10 μm thick, is made of nanoscale TiO_2 particles [188]

shown that TiO_2 films prepared with 10–20 nm size particles give extraordinary efficiencies for the conversion of incident photons into electric current, in some cases exceeding 90%. Photovoltaic devices with 18.2 mA/cm^2 photocurrent and overall light to electric energy conversion yield up to 10% under simulated AM 1.5 solar radiation (96.4 mW/cm^2) have been obtained.

Other sol-gel semiconducting materials may also be used. In a prelimanary work, Barros Filho et al. [189] have studied the UV action spectrum of 20–30 nm colloidal Nb_2O_5 particles and obtained promising results.

These new developments, which are somewhat outside the scope of this paper but for which the structure of the devices is quite similar to those of EC devices, appear to be extremely promising and the sol-gel process, once again, is one of the principal methods to be used to obtain outstanding coatings with specific functions.

7 Future Developments and Conclusion

Sol-gel processing of coatings for EC devices and other related systems like solar cells has been reviewed including report literature up to mid-1994. Up to few years ago most of the research has been concentrated on developing the

chemical processing of the sols in order to produce optically acceptable thin films and to show that these layers had the specific properties required for EC devices. Long term physical and electrochemical behavior, fundamental properties for technical applications, as well as microscopic studies of the phenomena have been rarely addressed. Nevertheless the good results obtained with the sol-gel processing has prompted more rigorous studies trying to fill these gaps and even complete devices have been tested in the last four years. Small size mirrors (up to 100 cm^2) are likely to be commercialized soon using at least one EC sol-gel layer. Devices with more than one sol-gel layer can be expected in the near future but more research and tests are necessary. Large scale devices such as smart windows require still more research in order to overcome the many technical difficulties encountered during the scale-up development.

From the physics and chemistry points of view there is a definite trend, observed in the last few years research, that the coatings which intercalate ions (H^+, Li^+, etc.) such as the EC and ion storage electrodes, or the coatings whose properties rely essentially on the attachment of specific molecules which modify their physical properties (mainly optical) under ambient stimuli (light, electric field, etc.), have to be made with colloidal nanoparticles linked together by some adequate thermal treatment. These coatings have quite high surface areas (up to several hundreds of square meters) which allows linking or binding of high amounts of ions or molecules to the active sites and a relatively high porosity allowing for diffusion of a large amount of ions (H^+, Li^+, etc.) On the other hand, due to their small thickness ($\leq$ μm) and nanoscale size of their constituents, these coatings retain adequate optical appearance. In this respect the sol-gel process is also definitively very promising as it allows preparation of the layers in a relatively simple and cheap way.

Another development which is also quite peculiar to the sol-gel process is the possibility of preparing hybrid organic-inorganic materials. This field is relatively new and has not yet been fully exploited for the development of such devices. The principal application should be in the realization of solid but still viscous electrolytes in order to substitute the polymeric or liquid systems in the 20–100 °C range.

We firmly believe that the future of the sol-gel process for the preparation of thin or thick layers for EC or related devices (such as solar cells) is bright with high probability of seeing, in the short to medium term, technical applications of high interest in these fields.

8 References

1. Lampert CM, Grandqvist CG (1990). In: Large-area chromogenics: materials and devices for transmittance control, SPIE IS4, 2, SPIE, Bellingham, Washington, USA
2. Lynam NR, Agrawal A (1990). In: Large-area chromogenics: materials and devices for transmittance control, SPIE IS4, 46, SPIE, Bellingham, Washington, USA

3. Cronin JP, Agrawal A (1994). In: Perspectives on glass science and technology. Symposium in honor of the 90th birthday of Prof. N. Kreidl, Triesenberg, Liechtenstein, to be published
4. Selkowitz SE, Lampert CM (1990). In: Large-area chromogenics: materials and devices for transmittance control, SPIE IS4, Optical Engineering Press, Bellingham, Washington, USA, 22
5. Selkowitz SC, Rubin M, Lee ES, Sullivan R (1994). In: Optical materials technology for energy efficiency and solar energy conversion XIII, SPIE 2255, 226, SPIE, Bellingham, Washington, USA
6. Reilly S, Arasteh D, Selkowitz SE (1991) Solar energy mater 1: 22
7. Agrawal M, Cronin JP, Zhang R (1992). In: Sol-gel optics II, SPIE, 1758, 300, SPIE, Bellingham, Washington, USA
8. Sullivan R, Lee ES, Papamichael K, Rubin M, Selkowitz S (1994). In: Optical materials technology for energy efficiency and solar energy conversion XIII, SPIE 2255, 443, SPIE, Bellingham, Washington, USA
9. Kraus T (1953) unpublished report (Balzers, Liechtenstein)
10. Deb SK (1969) Appl Opt Suppl 3: 192
11. Deb SK (1973) Phil Mag 27: 801
12. Inganäs O (1990). In: Large-area chromogenics: materials and devices for transmittance control, SPIE IS4, 328, SPIE, Bellingham, Washington, USA
13. Yang SC (1990). In: Large-area chromogenics: materials and devices for transmittance control SPIE IS4, 335, SPIE, Bellingham, Washington, USA
14. Grandqvist CG (1994) Solar energy materials and solar cells 32: 369
15. Czanderna AW, Lampert CA (1990) Solar Energy Research Institute SERT Golden, Col, USA TP 255-3637 U Category 316 DE 90000 334
16. Haas TE, Goldner RB (1990). In: Large-area chromogenics: materials and devices for transmittance control, SPIE IS 4, 170, SPIE, Bellingham, Washington, USA
17. Cronin JP, Tarico DJ, Tonazzi JCC, Agrawal A, Kennedy SR (1992). In: Sol-Gel Optics II, SPIE 1758, 343, SPIE, Bellingham, Washington, USA
18. Cronin JP, Tarico DJ, Tonazzi JCC, Agrawal A, Kennedy SR (1993) Solar energy materials and solar cells 29: 371
19. Chemseddine A, Morineau R, Livage J (1983) Solid State Ionics 9–10: 357
20. Xu G, Chen L (1988) Solid State Ionics 28–30: 1726
21. Judeinstein P, Livage J (1989) Materials Science and Engineering 133: 129
22. Yamamaka K (1981) Jpn J Applied Physics 20: 1307
23. Oi J, Kishimoto A, Kudo T (1992) J Solid State Chemistry 96: 13
24. Yamanaka K, Ohkawoto H, Kidon H, Kudo T (1986) Jpn J Applied Physics 25: 1420
25. Itoh K, Okamoto T, Wakita S, Niikura H, Murabayashi M (1991) Appl Organomet Chem 5: 295
26. Unuma H, Tonooka K, Suzuki Y, Furusaki T, Kodaira K, Matsushita T (1986) J Mat Lett 5: 1248
27. Takase A, Miyakawa K (1991) Jpn J Appl Phys Part 2 30: L1508
28. Bell JM, Green DC, Patterson A, Smith GB, MacDonald KA, Lee K, Kirkup LD, Cullen JD, West BO Apoccia L, Kenny MJ, Wilunski LS (1991) in: Opt. Mater. Technol. Energy Effic. Energy Convers. SPIE 1536, 29, SPIE, Bellingham, Washington, USA
29. Livage J (1992) Solid State Ionics 50: 307
30. Judeinstein P, Livage J (1991) J Mater Chem 1: 621
31. Craigen D, Mackintosh A, Hickman J, Colbow K (1986) J Electrochem Soc 133: 1529
32. Judeinstein P, Livage J (1990). In: Sol-Gel Optics – SPIE, Bellingham, Washington, USA, 1328, 344
33. Denesuk M, Cronin JP, Kennedy SR, Law KJ, Nielson GF, Uhlmann DR (1994). In: International Symposium on Optical materials technology for energy efficiency and solar energy conversion XIII, SPIE 2255, 52, SPIE Bellingham, Washington, USA
34. Joo SK, Raistrick JD, Huggins RA (1985) Solid State Ionics 17: 313
35. Göttsche J, Hinsch A, Wittwer P (1993) Solar Energy Materials and Solar Cells 31: 415
36. Yoshino T, Baba N, Yasuda K (1988) Nippon Kagaku Kaishi 9: 1525
37. Donnadieu A (1990) In: Large-Area Chromogenics: Materials and Devices for Transmittance Control, SPIE IS 4, 191, SPIE, Bellingham, Washington, USA
38. Wang B, Cheng J, Zhon W (1992) Huadong Huagong Xueynan Xuebao 18: 48
39. Moser FH, Lynam NR, US Patent (1989) 4, 855, 161
40. Stangar UL, Orel B, Grabec I, Ogoreve B, Kalcher K (1993) Solar Energy Materials and Solar Cells 31: 173

41. Orel ZC, Orel B (1994). In: Optical Materials Technology for Energy Efficiency and Solar Energy Conversion XIII, SPIE 2255, 285, SPIE, Bellingham, Washington, USA
42. Aegerter MA, LaSerra ER, Martins Rodrigues AC, Kordas G, Moore G, (1990). In: Sol-Gel Optics, SPIE 1328, 391SPIE, Bellingham, Washington, USA
43. Baudry P, Rodriguez ACM, Aegerter MA, Bulhões LOS (1990) J Non Crystal Solids 121: 319
44. Macedo MA, Dall'Antonia LH, Aegerter MA (1992). In: Sol-Gel Optics II – SPIE 1758, 320, SPIE, Bellingham, Washington, USA
45. Tonazzi JCL, Valla B, Macedo MA, Baudry P, Aegerter MA (1990). In: Sol Gel Optics, SPIE 1328, 375, SPIE, Bellingham, Washington, USA
46. Macedo MA, Dall'Antonia LH, Valla B, Aegerter MA (1992) J Non-Cryst Solids 147/148: 792
47. Macedo MA, Aegerter MA (1994) J Sol-Gel Science and Technology 2: 667
48. Valla B, Tonazzi JCL, Macedo MA, Dall'Antonia LH, Aegerter MA, Leones MAB, Bulhões LOS (1991) in: Optical Materials Technology for Energy Efficiency and Solar Energy Conversion X, SPIE 1536, SPIE, Bellingham, Washington, USA
49. Kéomany D, Poinsignon C, Deroo D (1995) Solar Energy Material and Solar Cells, 36: 397
50. Macedo MA (1994) PhD Thesis University of São Paulo
51. Ottaviani M, Panero S, Morzilli S, Scrosati B, Lazzari M (1986) Solid State Ionics 20: 197
52. Sata Y, Fujiwara R, Shimizu I, Inoue E (1982) Jpn J Appl Phys 21: 1642
53. Doeuff S, Sanchez C (1989) C R Acad Sci Ser 2309: 351
54. Nabavi M, Doeuff S, Sanchez C, Livage J (1989) Mater Sci Eng B3: 203
55. Ozer N, Chen DG, Simmons JH (1991) Ceram Trans Glasses Electron Appl 20: 253
56. Ozer N, Tepehan F, Bozkurt N (1992) Thin Solid Films 219: 193
57. Bell JM, Barczynska J, Evans LA, MacDonald KA, Wang J, Green DC, Smith GB (1994). In: Optical materials technology for energy efficiency and solar energy conversion XIII, SPIE 2255, 324, SPIE, Bellingham, Washington, USA
58. Hagfeld A, Vlachopoulos N, Gilbert S, Grätzel M (1994). In: Optical materials technology for energy efficiency and solar energy conversion XIII, SPIE 2255, 297, SPIE, Bellingham, Washington, USA
59. Stangar UL, Orel B, Hutchins MG (1994). In: Optical materials technology for energy efficiency and solar energy conversion XIII, SPIE 2255, SPIE, Bellingham, Washington, USA, 261
60. Orel B, Stangar UL, Hutchins MG, Kalcher K (1994) J Non Cryst Solids 175: 251
61. Reichman B, Bard AJ (1980) J Electrochem Soc 127: 241
62. Yu PC (1991) Thesis, Tufts University, Dept. of Chemistry
63. Gomes MAB, Bulhões LOS, Castro SC, Damião AJ (1990) J Electrochem Soc 137(10): 3067
64. Gomes MAB, Bulhões LOS (1990) Electrochim. Acta 35(4): 765
65. Alves MC (1989) MSc Thesis, Federal University of São Carlos (Brazil)
66. Lee RG, Crayston JA (1991) J Mater Chem 1: 381
67. Faria RC, Bulhões LOS (1994) J Electrochem Soc 141: L29
68. Avellaneda CO, Macedo MA, Aegerter MA (1994). In: Proc. 38o. Congresso Brasileiro de Cerâmica, 109 Blumenau, SC
69. Ozer N, Barreto R, Büyüklinanl T, Lampert C (to be published) Solar Energy Materials and Solar Cells
70. Aegerter MA (1991) Patent pending No WO 91/02282 (PCT/BR90/00006)
71. Avellaneda CO, Macedo MA, Florentino AO, Barros Filho DA, Rabelo AA, Aegerter MA (1994). In: Proc 2nd conference "Sociedade brasileira de pesquisadores nikkeis", São Paulo, 17
72. Aegerter MA, Avellaneda CO (to be published). In: International Symposium on Sol-Gel Science and Technology, ACERS Pacific Coast Meeting, Los Angeles, USA
73. Avellaneda CO, Macedo MA, Florentino AO, Barros Filho DA, Aegerter MA (1994). In: Sol Gel Optics III, SPIE 2288, 422, Bellingham, Washington, USA
74. Avellaneda CO, Macedo MA, Florentino AO, Aegerter MA. In: Optical materials technology for energy efficiency and solar energy conversion XIII, SPIE 2255, 38, SPIE, Bellingham, Washington, USA
75. Cogan SF, Rauh RD, Plante TD, Nguyen NM, Westwood JD (1980). In: Physical electrochemistry division, The electrochemical society electrochromic materials, Pennington, New Jersey, 99
76. Talledo A, Andersson AM, Granqvist CG (1990) J Mater Res 5: 1253
77. Nabavi M, Sanchez C, Livage J (1991) Eur J Solid State Inorg Chem 28: 1173
78. Sanchez C (1992) Bol Soc Esp Ceram Vidrio 31: 191
79. Yoshino T, Baba N, Kouda Y (1987) Jpn J Appl Phys 26: 782

80. Desilvestro J, Haas O (1990) J Electrochem Soc 137: 50
81. Bach S, Pereira-Ramos JP, Baffier N, Messina R (1990) J Electrochem Soc 137: 1042
82. Pereira-Ramos JP, Messina R, Bach S, Baffier N (1990) Solid State Ionics 40–41: 970
83. Amarilla J-M, Casal B, Galvan J-C, Ruiz-Hitzky E (1992) Chem Mater 4: 62
84. Nagase K, Shimizu Y, Miura N, Yamazoe N (1993) J Ceram Soc Jpn 101: 1032
85. Hackwood S, Dayem AH, Beni A (1982) Phys Rev B 26: 471
86. Agrawal A, Habib HR, Agrawal RK, Cronin JP, Roberts DM, Popwich R-C, Lampert CM (1992) Thin Solid Films 221: 239
87. Svensson JSEM, Granqvist CG (1980) App Phys Lett 49: 1568
88. Lampert CM, Omstead TR, Yu PC (1985). In: SPIE, 562, 15, SPIE, Bellingham, Washington, USA
89. Miles MH, Stilwell DE, Hollins RA, Henry RA (1980). In: Physical electrochemistry division, The electrochemical society electrochromic materials, Pennington, New Jersey, 137
90. Gottesfeld S (1980) J Electrochem Soc 127: 272
91. Moser FH, Lynam NR (1990) US Patent, 4, 959, 247
92. Orel B, Macek M, Svege F, Kalcher K (1994) Thin Solid Films (in press)
93. Orel B, Macek M, Surca A (1994). In: Optical materials technology for energy efficiency and solar energy conversion XIII, SPIE 2255, 273, SPIE, Bellingham, Washington, USA
94. Olivi P, Pereira EC, Longo E, Varella JA, Bulhões LO (1993) J Electrochem Soc 140: L81
95. Chopra KL, Major S, Pandya DK (1983) Thin Solid Films 102: 1
96. Haacke G (1977) Ann Rev Mater Sci 7: 73
97. Lynam NR (1980). In: Physical electrochemistry division, the electrochemical society electrochromic materials, Pennington, New Jersey, 201
98. Arfsten NJ (1984) J Non-Cryst Solids 63: 243
99. Arfsten NJ, Kaufman R, Dislich H (1984). In: Ultrastructural processing of ceramics, glasses and composites, 189, Wiley Interscience Publishers, New York
100. Takahashi Y, Hayashi H, Dhya Y (1992). In: Better Ceramics Through Chemistry V, MRS 271, 401
101. Takahashi Y, Wada Y (1990) J Electrochem Soc 137: 267
102. Gonzalez-Oliver GJR, Kato I (1986) J Non-Cryst Solids 82: 400
103. Brinker CJ, Scherer GW (1990). In: Sol-gel science: the physics and chemistry of sol-gel processing, Academic Press (ed) San Diego, 787p
104. Brinker CJ, Hurd AJ, Frye GC, Ward KJ, Ashley CS (1990) J Non-Cryst Solids 121: 294
105. Tsunashima A, Yoshimizu H, Kodaira K, Shimada S, Matsushito F (1986) J Mater Sci 21: 2731
106. Hiratsuka RS, Pulcinelli SH, Santilli CV (1990) J Non-Cryst Solids 121: 76
107. Maddalena A, DalMaschio R, Diré S, Raccanelli A (1990) J Non-Cryst Solids 121: 365
108. Goodman FJ, Gregg SJ (1960) J Chem Soc 237: 1162
109. Giesekke EW, Gutowsky HS, Kirkov P, Laitineu HA (1967) Inorg Chem 6: 1269
110. Orel B, Stanger UL, Crnjak-Orel Z, Bakovec P, Kosec M (1994) J Non-Cryst Solids 167: 272
111. Cocco G, Enzo S (1987) Mater Chem Phys 17: 541
112. Pozarnsky GA, Wright L, McCormick AV (1994) J Sol-Gel Science and Technology 3: 57
113. Lynam NR, Moser FH, Hichwa BP (1987). In: SPIE, 130
114. Hajimoto Y, Matsushima M, Ogura S (1979) J Electron Mater 8: 301
115. Uchikawa K, Niwa T (1987) US Patent 4, 652, 090
116. Ling HC, Yang MF, Rhodes WW (1986). In: Science of ceramic chemical processing, John Wiley and Sons, 285
117. Ozer N, He Y, Lampert CM (1994). In: Optical materials technology for energy efficiency and solar energy conversion XIII, SPIE 2255, 456, SPIE, Bellingham, Washington, USA
118. Howe AT, Sheffield SH, Childs PE, Shilton MG (1980) Thin Solid Films 67: 415
119. Takahashi T, Tanase S, Yamamoto O (1980) J Appl Electrochem 10: 415
120. Charbouillot Y, Ravaine D, Armand M, Poinsignon C (1988) J Non-Crystal Solids 103: 325
121. Judeinstein P, Livage J, Zarndiansky A, Rose R (1988) Solid State Ionics 28–30: 1722
122. Sanchez JY, Denoyelle A, Poinsignon C (1993) Polym Adv Technol 4: 89
123. Huggins RA (1977) Electrochim Acta 22: 773
124. Goldner RB, Haas TE, Seward G, Wong KK, Norton P, Foley G, Berera G, Wei G, Schulz S, Chapman R (1988) Solid State Ionics 28–30: 1715
125. Oi T, Miyauchi K (1981) Mater Res Bull 16: 1281
126. Raistrick ID, Ho C, Huggins RA (1976) Mater Res Bull 11: 953
127. Klein LC (1988) Sol-Gel Technology for Thin Films, Fibers, Preforms, Electronics and Specialty Forms, Noyes Publications (ed) New Jersey, USA, 407p

128. Aegerter MA, Jafelicci Jr. M, Souza DF, Zanotto ED (1989) Sol-Gel Science and Technology, World Scientific (ed) Singapore, 505p
129. Sakka S, Yoko T (1992). In: Chemistry, spectroscopy and applications of sol-gel glasses, Springer-Verlag Berlin, 89
130. Schmidt H (1992). In: Chemistry, spectroscopy and applications of sol-gel glasses, Springer-Verlag Berlin, 119
131. Agrawal A, Cronin JP, Zhang R (1993) Solar Energy Materials and Solar Cells 31: 9
132. Morineau R (1985) Vide, Couches Minces 40: 281
133. Uhlmann DR, Boulton JM, Teowee G, Weisenbach L, Zelinski BJ (1990). In: Sol-gel, SPIE 1328, 270, SPIE, Bellingham, Washington, USA
134. Livage J (1988) Chem Sci 28: 9
135. Habib MA, Glueck D (1989) Solar Energy Materials 18: 127
136. Göttsche J, Hinsch A, Wittwer V (1993). In: Large-area chromogenics: Materials and devices for transmittance control, SPIE IS4, 13, SPIE, Bellingham, Washington, USA
137. Nabavi M, Sanchez C (1990) C R Acad Sci Paris 310 – série II: 117
138. Mehrotra RC (1988) J Non-Cryst Solids 100: 1
139. Atkinson A, Guppy RM (1991) J Mater Sci 26: 3869
140. Makishima A, Kubo H, Wada K, Kitami Y, Shimohira T (1986) J Am Ceram Soc 69: C127
141. Giuntini JC, Granier W, Zanchetta TV, Taha A (1990) J Mater Sci Lett 9: 1383
142. Grandqvist CG (1993) Sol State Ionics 60: 213
143. Zea Bermudes VD, Baril D, Sanchez JY, Armand M, Poinsignon C (1992). In: Optical materials technology for energy efficiency and solar energy conversion XI: Chromogenics for Smart Windows, SPIE 1728, 180, SPIE, Bellingham, Washington, USA
144. Tatsumisago M, Kishida K, Minami T (1993) Solid State Ionics 59: 171
145. Boilot JP, Colomban P (1988). In: Sol-gel technology for thin films, fibers, preforms, electronics and specialty shapes, Noyes Publications, 303
146. Klein LC, Ho SF, Szu SP, Greenblatt M (1991). In: Applications of Analytical Techniques to the Characterization of Materials, Plenum Press, New York, 101
147. Klein LC (1993). In: CNRS European sol-gel summer school, Château de Bierville, France, 147
148. Hayri EA (1989) J Non-Cryst Solids 94: 167
149. Smaihi M, Petit D, Gourbillean F, Chaput F, Boilot JP (1991) Solid State Ionics 48: 213
150. Bozano D, Aegerter MA (1994) Private Communication
151. Wang B, Szu S, Greenblatt M, Klein CC (1992) Chem Mater 4: 191
152. Wang B, Szu S, Greenblatt M, Klein LC (1992) Solid State Ionics 53/56: 1214
153. Kuwano J, Naito Y, Kato M (1987) Yogyo Kyo Kaishi 95: 176
154. Hayri EA, Greenblatt M (1987) J Non-Cryst Solids 94: 387
155. Wang B, Szu S, Greenblatt M, Klein CC (1991) Solid State Ionics 47: 297
156. Wang B, Szu S, Greenblatt M, Klein LC (1992). In: The physics of non-crystalline solids, 203, Taylor & Francis London
157. Wang B, Greenblatt M, Yan J, Wu Y (1994) J Sol-Gel Science and Technology 2: 323
158. Ogasawara T, Klein LC (1994) J Sol-Gel Science and Technology 2: 611
159. Trifonova V (1994) J Sol-Gel Science and Technology 2: 447
160. Judeinstein P, Titman J, Stamm M, Schmidt H (1994) Chem Mater 6: 127
161. Macedo MA, Dall'Antonia LH, Aegerter MA (1992). In: Smart Materials Fabrication and Materials for Micro-Electro-Mechanical Systems MRS, 276, 125
162. Oihshi T, Maekawa S, Kato A (1992) Jpn Kokai Tokkyo Koho JP 04 242226 A2 920828 Heisi
163. Takahashi T, Nomura S (1993) Jpn Kokai Tokkyo Koho JP 05 177757 A2 930720 Heisei
164. Kaufman VR, Levy D, Avnir D (1986) J Non-Cryst Solids 82: 103
165. Levy D, Avnir D (1988) J Phys Chem 92: 4734
166. Levy D, Sinhorn S, Avnir D (1989) J Non-Cryst Solids 113: 137
167. Matsui K, Moroboshi T, Yoshida S (1989). In: MRS Int Meet Adv Mat, 12, 203
168. Preston D, Pouxviel JC, Novison T, Kaska W, Dunn B, Zink JI (1990) J Phys Chem 94: 4167
169. Nogami M, Sugiura T (1993) Mat Sci Lett 12: 1544
170. Yamamaka SA, Zink JI, Dunn B (1992). In: Sol-Gel Optics II, SPIE, 372
171. Ueda M, Kim HB, Ikeda T, Ichimara K (1992) Chem Mater 4: 1229
172. Ueda M (1993) J Non-Cryst Solids 163: 125
173. Hou L, Mennig M, Schmidt H (1994). In: Optical materials technology for energy efficiency and solar energy conversion XIII, SPIE 2255, 26, SPIE, Bellingham, Washington, USA
174. Hou L, Hoffmann B, Mennig M, Schmidt H (1994) J Sol-Gel Science and Technology 2: 635

175. Judeinstein P (1994) J Sol-Gel Science and Technology 2: 147
176. Mennig M, Krug H, Fink-Straube C, Oliveira PW, Schmidt H (1992). In: Sol-Gel Optics II, SPIE 1758, 387, SPIE, Bellingham, Washington, USA
177. Adler M (1968) Rev Mod Phys 40: 714
178. Geffcken W (1939). In: Jenaer Glaswerk Schott and Gen., Jena (ed) 411 (GDR Patent, 736)
179. Schroeder H (1962) Opt Acta 9: 249
180. Schroeder H (1969) Phys Thin Films 5: 87
181. Potember RS, Speck KR (1990). In: Sol-Gel Optics, SPIE 1328, 364 SPIE, Bellingham, Washington, USA
182. Levy D, Serna CJ, Oton JM (1991) Mat Letters 10: 470
183. Oton JM, A. Serrano A, Serna CJ, Levy D (1991) Liq Cryst 10: 733
184. Levy D, Serna CJ, Serrano A, Vidal J, Oton JM (1992). In: Sol-Gel Optics II, SPIE 1758, 476 SPIE, Bellingham, Washington, USA
185. Levy D, Quintana X, Covadonga R, Otón JM (1985). In: Sol-Gel Optics III, SPIE 2288, 529, Bellingham, Washington, USA
186. Levy D, Serrano A, Otón JM (1994) J Sol-Gel Science and Technology 2: 803
187. Graetzel M (1993) MRS Bulletin XVII 10: 61
188. Graetzel M (1994) J Sol-Gel Science and Technology 2: 673
189. Barros Filho DA, Maĉedo MA, Florentino A, Aegerter MA (1994). In: Proc. Congresso Brasileiro de Cerâmica, Blumenau, SC, Brasil, p 80